Affinity and its derivatives in the glass transition process

Jean-Luc Garden, Hervé Guillou, Jacques Richard, L. Wondraczek

Affinity and its derivatives in the glass transition process

J.-L. Garden,* H. Guillou, and J. Richard

Institut Néel, CNRS et UJF, 25 Avenue des Martyrs, 38042 Grenoble cedex 09, France

L. Wondraczek

Departement of Materials Science, Chair of Glass and Ceramics,

University of Erlangen-Nuernberg, 91058 Erlangen, Germany

Abstract

The thermodynamic treatment of the glass transition remains an issue of intense debate. When associated with the formalism of non-equilibrium thermodynamics, the lattice-hole theory of liquids can provide new insight in this direction, as has been shown by Schmelzer and Gutzow [J. Phys. Chem. **125**, 184511 (2006)], by Möller et al. [J. Phys. Chem. **125**, 094505 (2006)], and more recently by Tropin et al. [J. Non-Cryst. Solids **357**, 1291; 1303 (2011)]. Here, we employ a similar approach. We include pressure as an additional variable, in order to account for the freezing-in of structural degrees of freedom upon pressure increase. Secondly, we demonstrate that important terms concerning first order derivatives of the affinity-driving-force with respect to temperature and pressure have been previously neglected. We show that these are of crucial importance in the approach. Macroscopic non-equilibrium thermodynamics is used to enlighten these contributions in the derivation of C_p, κ_T, and α_p. The coefficients are calculated as a function of pressure and temperature following different theoretical protocols, revealing classical aspects of vitrification and structural recovery processes. Finally, we demonstrate that a simple minimalist model such as the lattice-hole theory of liquids, when being associated with rigorous use of macroscopic non-equilibrium thermodynamics, is able to account for the primary features of the glass transition phenomenology. Notwithstanding its simplicity and its limits, this approach can be used as a very pedagogical tool to provide a physical understanding on the underlying thermodynamics which governs the glass transition process.

*Electronic address: jean-luc.garden@grenoble.cnrs.fr

I. INTRODUCTION

There are numerous approaches dealing with the glass transition process. Some are based on microscopic models, while others are mostly driven by macroscopic and phenomenological view-points. One of this approaches, is the thermodynamic of irreversible processes, or non-equilibrium thermodynamics. Within this latter approach, the notion of one or more structural order parameters is used to characterize the glassy state. Such structural order parameters ξ_i, have to be taken into account in addition to classical thermodynamic variables in order to describe the non-equilibrium aspect of the glass transition. The affinity A is the conjugated variable associated to the order parameter. It plays a fundamental role since it defines the driving force of the non-equilibrium process. The formalism of classical non-equilibrium thermodynamics has been developed by De Donder in a self-consistent manner [1]. The first attempts to apply this theory to glass science have been made by Prigogine and Defay[2], and Davies and Jones [3].

Non-equilibrium thermodynamics has been used all along the last century by different groups of researchers, and has seen renewed interest in the last few years [4–15]. As an example, Bouchbinder and Langer used the generalized non-equilibrium thermodynamics based on internal variables to investigate one of the most striking aspect of the glass transition, i.e. the Kovacs effect [16]. They provided fits of the numerical simulation curves obtained by Mossa and Sciortino on the Kovacs effect [17]. Among these recent works, Gutzow, Schmelzer and co-workers have brought new aspects to the field [18–24]. Using the so-called lattice-hole theory of liquids, and an evolution equation for the order parameter as a function of temperature, they investigated the process of vitrification and structural recovery following defined temperature protocols [18, 19, 23, 24]. Among other points, a new expression for the Prigogine-Defay ratio and a thermodynamic definition of the fictive temperature was provided [18, 24].

In this paper, we elaborate the same approach towards a more complete and rigorous treatment of the glass transition. First, we include pressure as an additional variable into the expression of the relaxation time to account for vitrification by pressure perturbation in analogy to temperature changes. Secondly, we demonstrate that the total derivatives of the affinity with respect to pressure and temperature are of crucial importance for the consistency of the approach. We show that to neglect them leads to incoherence such as

discussed later.

The paper is organized as follows: In the section II, the lattice-hole theory of liquids is recalled. The configurational Gibbs free energy is written as a function of pressure p, temperature T, order parameter ξ and phenomenological parameters. Next, we illustrate how to extract the values of the phenomenological parameters from experimental data. Then we compute the equilibrium values of the order parameter as a function of temperature and pressure.

In section III, we describe how to obtain the non-equilibrium behavior of the order parameter assuming a first order relaxation equation with a modified Vogel-Fulcher-Tamman-(VFT) relaxation time accounting for the pressure and the temperature. In resolving numerically the relaxation equation, we are able to compute the non equilibrium values of the order parameter according to specified temperature and pressure variation protocols.

In section IV, we use these results to compute the affinity as a function of temperature or pressure. We compute the configurational parts of the thermodynamic coefficients C_p, κ_T, α_p and show that in order to obtain qualitative agreement with experimental observations, the derivatives of the affinity should not be neglected (as done in, e.g., Ref. [24]). This model is able to qualitatively reproduce typical experimental observations such as for instance vitrification and structural recovery.

In the final section V, we discuss the fictive temperature concept and its possible model-independent definition within this framework.

It will be demonstrated that a simple minimalist model such as the lattice-hole theory of liquids, when being associated with rigorous use of macroscopic non-equilibrium thermodynamics is able to account for the primary features of the glass transition phenomenology. Because of this simplicity, this approach can be used as a very pedagogical tool to tackle the thermodynamics which underlies glass transition process.

II. EQUILIBRIUM LATTICE-HOLE MODEL OF LIQUIDS

A. Introduction of the lattice-hole model of liquids

The phenomenological approach of the glass transition by the lattice-hole model has been described in several papers [25, 26] and books [27, 28]. Generally, liquids have a larger molar

volume than solids. Thus some volume of the liquid is supposed to embed holes. Let be $\mathcal{N}_A$ the Avogadro number and N_h the number of holes per mole of the liquid. In the lattice-hole model this defines an order parameter ξ :

$$\xi = \frac{N_h}{\mathcal{N}_A + N_h}.$$

A perfect crystal has no holes and $\xi = 0$.

A liquid at equilibrium at a given temperature T and pressure p has a given excess volume with respect to the crystal form $\triangle V_{conf} = V_{liq}(T,p) - V_{crystal}(T,p)$ from which the equilibrium value of the order parameter can be measured if the relationship between excess volume (or configurational volume) and ξ is known. Following previous approaches [18, 19, 28], we assume constant volume of holes v_0. The excess volume and the order parameter are thus connected by the following relationship :

$$\triangle V_{conf} = N_h v_0 = V_0 \frac{\xi}{1-\xi} \tag{1}$$

where V_0 is the molar volume of one hole. In one of the first hole theories Frenkel considered the holes to be atom-sized [27] while later Hirai and Eyring considered them to be much smaller [29].

The configurational molar Gibbs free energy associated with the presence of holes in the liquid is written as [28]:

$$\triangle G_{conf} = \Delta E_0 \xi + p V_0 \frac{\xi}{1-\xi} + RT \left[\ln(1-\xi) + \frac{\xi}{1-\xi} \ln \xi \right]. \tag{2}$$

In this expression of the configurational Gibbs free energy, discussed thoroughly in the monograph [28], ΔE_0 represents the energy associated with the braking of molecular bonds between the material molecules in order to create one mole of holes. The last term in the right hand side of the equation corresponds to the entropy of mixing between holes and molecules. The value ΔE_0 and V_0 can be extracted from experimental data as described in the next paragraph.

1. *Extraction of ΔE_0 and V_0:*

The lattice-hole model is used up to the melting temperature T_m. We use experimental measurements at T_m of ΔV_m and ΔS_m in order to calculate ΔE_0 and V_0. As an exemplary model system, we choose *o*-terphenyl for which PVT measurements, and melting data

Table I: Characteristic of *o*-terphenyl melting and corresponding parameters used in the lattice-hole model.

p (MPa)	0.1	39.2	78.5
T_m(K)	329.352	343.4	356.8
ΔS_m ($\mathrm{J \cdot K^{-1} \cdot Mol^{-1}}$)	52.195	51.61	50.87
V_l ($\mathrm{cm^3 \cdot Mol^{-1}}$)	218.50	215.87	213.51
V_c ($\mathrm{cm^3 \cdot Mol^{-1}}$)	199.13	197.83	196.61
ΔV_m ($\mathrm{cm^3 \cdot Mol^{-1}}$)	19.38	18.03	16.90
$\xi_{eq}(T_m)$	0.09279	0.087209	0.082433
V_0 ($\mathrm{cm^3 \cdot Mol^{-1}}$)	7.34	7.08	6.89
ΔE_0 ($\mathrm{J \cdot Mol^{-1}}$)	7908.9	8081.3	8252.3

at different pressures, are available [30]. A relaxation time constant $\tau(p,T)$ depending on temperature as well as pressure, is also available from experimental data [31]. The characteristics of the melting process are recalled in the table I. From these experimental values we derive the parameters used to describe the lattice-hole model.

First, we estimate the equilibrium value of the order parameter at the melting temperature T_m . We express the Eq. (1) at T_m and invert it :

$$\xi_{eq}(T_m) = \frac{\Delta V_{conf}/V}{(1 + \Delta V_{conf}/V)},$$

where $V = (V_l + V_c)/2$ is taken as an initial estimation of V_0 and $\Delta V_{conf} = V_l - V_c$. The computed values of ξ_{eq} are presented in the table I. Once an approximate value for ξ_{eq} is known, the estimation of V_0 and ΔE_0 is done as following.

The Eq. (2) is valid at the melting temperature of the crystal. The liquid-crystal transition is an equilibrium phase transition and thus the affinity $A = 0$:

$$A = -\left.\frac{\partial \Delta G_{conf}}{\partial \xi}\right|_{T,p} = 0. \tag{3}$$

This conditions is rewritten as :

$$-RT_m \ln \xi_{eq} = \Delta E_0 (1 - \xi_{eq})^2 + p_m V_0. \tag{4}$$

The various (T_m, p_m, ξ_{eq}) are known from experimental works [30] and from the basic equation of state (Eq. (4)).

To completely solve the system we need a third equation that is obtained considering the equilibrium melting transition. The Clausius-Clapeyron equation describing the line of coexistence of the crystal and liquid phases in the $p-T$ plane allows to write [32]:

$$\frac{dT}{dp} = \frac{T\left(\partial \triangle V_{conf}/\partial\xi\right)_{T,p}}{\left(\partial \triangle H_{conf}/\partial\xi\right)_{T,p}}. \tag{5}$$

Where $\triangle H_{conf} = \Delta E_0 \xi + pV_0\xi/(1-\xi)$ is the configurational enthalpy. The various configurational parts are expressed at T_m and p_m from Eq. (1) and equation of $\triangle H_{conf}$ above:

$$\frac{\partial \triangle V_{conf}}{\partial \xi} = \frac{V_0}{(1-\xi)^2} \tag{6}$$

$$\frac{\partial \triangle H_{conf}}{\partial \xi} = \Delta E_0 + \frac{pV_0}{(1-\xi)^2} \tag{7}$$

Combining Eq. (4) and Eq. (6) and (7) at p_m and T_m, Eq. (5) is rewritten as :

$$\frac{dT}{dp} = -\frac{V_0}{R\ln\xi_{eq}(T_m,p_m)} = \frac{\Delta V_m}{\Delta S_m}. \tag{8}$$

The experimental values for ΔV_m and ΔS_m allow to compute the value of V_0 (see Table I). It is then possible to give an approximate value for ΔE_0 by using Eq. (4). These values are slightly pressure dependent, but as we are only interested in general behavior, we use the values of V_0 and ΔE_0 obtained at atmospheric pressure, to compute the properties of the system at various pressures and temperatures.

We compute the equilibrium values of the order parameter, ξ_{eq}, for various pressures and temperatures by solving Eq. (3). The evolution of ξ_{eq} as a function of temperature and at constant pressure is plotted on the inset (a) of Fig. (1) and the evolution of ξ_{eq} as a function of pressure and at constant temperature is plotted on the inset (a) of Fig. (2). In both cases ξ_{eq} continuously changes and shows no saturation in the temperature and pressure intervals investigated. At equilibrium, the system continuously adapts its configuration so as to minimize its Gibbs free energy according to the external set of constraints, here imposed only by the temperature T and pressure p.

III. OUT OF EQUILIBRIUM PROPERTIES OF THE LATTICE-HOLE MODEL OF LIQUIDS

A. Rate equation

From the knowledge of $\xi_{eq}(p,T)$ the changes of the order parameter $\xi(p,T,t)$ upon temperature variation $T(t)$, pressure variation $p(t)$, or both, is computed by solving the following first order equation :

$$\frac{d\xi(T,p,t)}{dt} = \frac{(\xi_{eq}(T,p) - \xi(T,p,t))}{\tau(T,p)}. \tag{9}$$

The initial condition should be a state in the liquid at equilibrium uniquely determined by the values of T and p. The equation (9) assumes that the linear regime holds (see discussion on this point in Ref. [19]) and that the relaxation time of the order parameter depends only on T and p.

Equations (4) and (9) together with the expression (10) of the relaxation time below entirely determine the out of equilibrium properties of the system.

B. Extraction of $\tau(T,p)$

The question now arises as to how the melt could freeze. From the relaxation law (Eq. (9)) the glass transition takes place if the system is brought within an appropriate time scale in a range of variables (p,T) where the relaxation time τ is high enough that $\frac{d\xi}{dt}$ tends towards zero. In this case, all configurational contributions to the thermodynamic properties disappear. Generally, the expressions of the relaxation time that are chosen follow the so-called VFT law, $\tau = A\exp\left(\frac{A}{T-T_0}\right)$ or Tool–Narayanaswamy–Moynihan (TNM) law $\tau(T,T_f) = A\exp\left[x\frac{\triangle h^*}{RT} + (1-x)\frac{\triangle h^*}{RT_f}\right]$. In this work, a modified VFT law with pressure is considered for the relaxation time :

$$\tau = \tau_0 \exp\left(\frac{B + b(p-0.1)}{T - [T_0 + a(p-0.1)]}\right) \tag{10}$$

where p is in MPa and $B = 2500$ K; $b = 0.29$ K/MPa; $a = 0.3$ K/MPa; $T_0 = 191$ K; $\tau_0 = 8.9 \times 10^{-19}$s. This expression is taken from the results in Leyser *et al.*[31] who fitted specific-heat spectroscopy data both in pressure and temperature. The evolution of τ on the investigated temperature interval is shown in the inset (b) of Fig. (1) and the evolution of τ on the investigated pressure interval is shown in the inset (b) of Fig. (2).

parameters	V_0	ΔE_0	τ_0	B	b	T_0	a
value	$7.3383\ \mathrm{cm}^3 \cdot \mathrm{Mol}^{-1}$	$7909\mathrm{J} \cdot \mathrm{Mol}^{-1}$	$8.9 \cdot 10^{-19}\,\mathrm{s}$	$2500\,\mathrm{K}$	$0.29\ \mathrm{K{\cdot}MPa}^{-1}$	191 K	$0.3\,K \cdot \mathrm{MPa}^{-1}$

Table II: Table of the parameters used for the numerical computations used in this work.

C. Temperature dependence of ξ

We check if the system is driven out of equilibrium and frozen by changing the temperature. The evolution of the order parameter is numerically computed by using Eq. (9) and the expression (10) for the relaxation time τ. The initial condition starts from equilibrium in the liquid phase at pressure $p_0 = 0.1\,\mathrm{MPa}$ and $T_{max} = T_m = 329.35\,\mathrm{K}$. While the pressure is kept constant, the temperature is decreased at a defined rate $\gamma_T = dT/dt$ until temperature $T_{min} = 230$ K. Obviously the choice of such minimum temperature is arbitrary: we only ensure to have freezing (ξ =constant) conditions at this temperature. Subsequently, the system is reheated at the same rate until the initial equilibrium state. Fig. (1) shows the evolution of ξ as a function of temperature T obtained for two different rates $\gamma_T = \pm 6\,\mathrm{K/min}$ and $\gamma_T = \pm 0.3\,\mathrm{K/min}$. The plots for cooling and subsequent heating are shown. Upon cooling, the departure from equilibrium occurs at different temperatures and depends on the cooling rate. The higher the cooling rate, the higher is the temperature at which the system departs from equilibrium. The glass transition temperature is around $T_g = 245$ K close to the value reported in Ref. [30] for the same cooling protocol. The ratio of the glass transition temperature and the melting temperature is $\theta = T_g/T_m = 0.74$ is slightly higher than the value of 2/3 of the Kauzmann-Beaman rule [28]. These results, in quantitative agreements with experiments, suggest that the parameters used in the expression of the relaxation time are physically relevant.

Upon reheating, the order parameter ξ first crosses the equilibrium value ξ_{eq} before returning to the equilibrium curve although with some delay. This behavior is well understood and has been obtained and discussed in Ref. [19]. The behavior of the order parameter upon reheating is due to the rapid decrease of the relaxation time. At a particular point the system reaches equilibrium $\xi = \xi_{eq}$ and would stay there if the temperature was kept constant (see Eq. (9)). However, the temperature keeps increasing at a constant rate and the system relaxation time is not yet sufficiently fast to follow the temperature variation. Thus, the

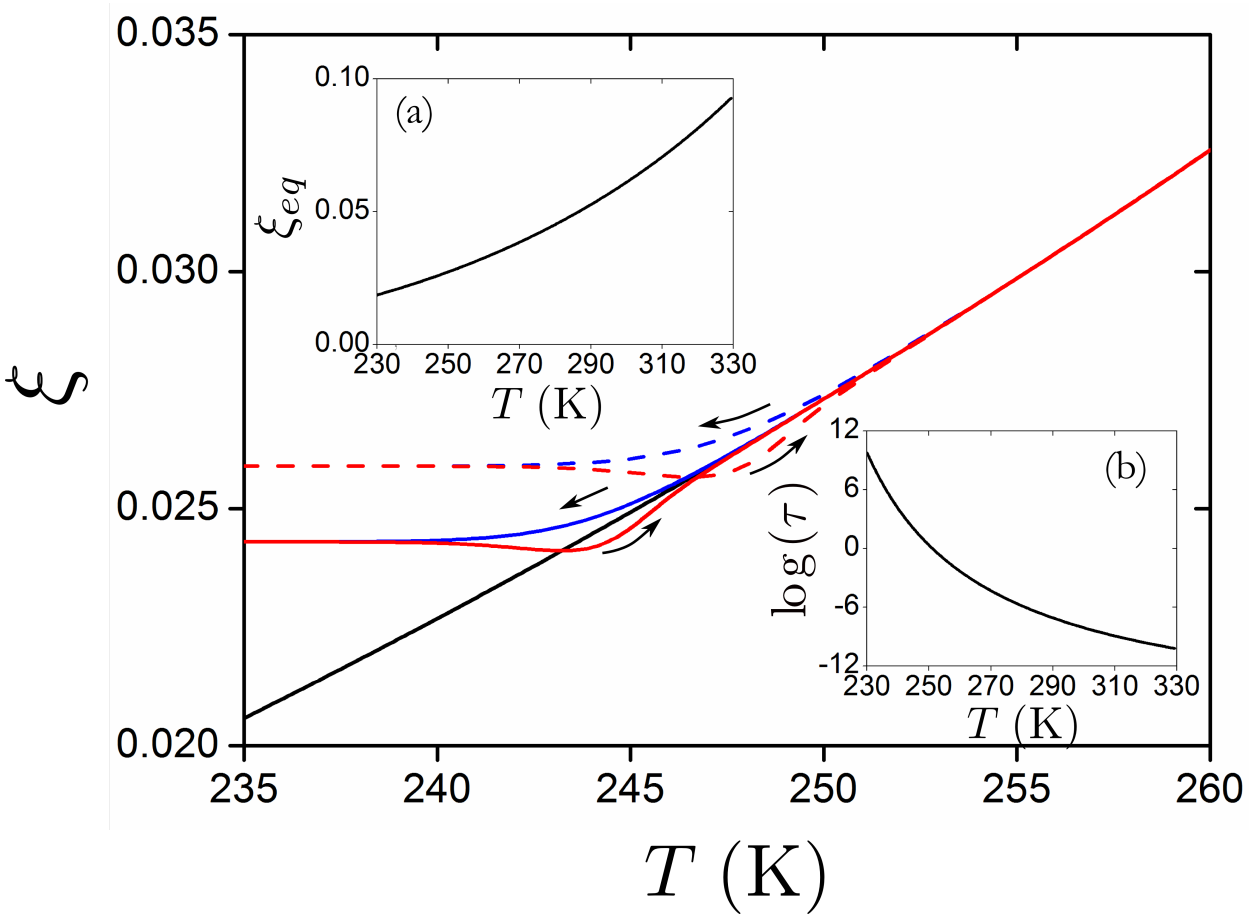

Figure 1: Evolution of the order parameter as a function of temperature at constant pressure $p = 0.1\,\mathrm{MPa}$. The arrows and colors indicate the sense of variation of the temperature : down and blue correspond to cool down and vitrification whereas up and red correspond to reheating. The temperatures variation rates are $\gamma_T = \pm 0.3$ K/min (thick lines) and $\gamma_T = \pm 6$ K/min (dashed lines). *Insets :* (a) Equilibrium order parameter as a function of temperature on the whole temperature range. (b) Evolution of $\log(\tau)$ as a function of temperature.

system is again driven out of equilibrium until the relaxation time becomes sufficiently small as compared to the temperature variation time that can be connected to the inverse of the rate γ_T^{-1}. Then the system returns to equilibrium.

D. Pressure dependence of ξ

We check if the system is driven out of equilibrium and frozen by changing the external pressure. We start the numerical computations from an initial condition in an equilibrium state at pressure $p_0 = 0.1\,\mathrm{MPa}$ and $T_0 = 271.6\,\mathrm{K}$. While the temperature is kept constant, the pressure is raised at a rate $\gamma_p = dp/dt$ until a maximum value of $p_{max} = 200\,\mathrm{MPa}$ is reached. The pressure is then reduced at the rate $-\gamma_p$ until the initial equilibrium state. The evolution of the order parameter is numerically computed by using equation (9) and the expression (10) for the relaxation time τ. The figure (2) shows the results obtained for two different rates $\gamma_p = 25\,\mathrm{MPa/min}$ and $\gamma_p = 1.25$ MPa/min. The plots of the values of the order parameter for pressure increase and subsequent decrease are shown together with the equilibrium value of the order parameter as a function of pressure. It is observed that the system undergoes a glass transition as the pressure is increased. The curves are very similar to those shown in Fig. (1). The effect of the pressure variation rates on the transition pressure is observed: at a higher rate the pressure at which the system is frozen is smaller than at a smaller rate. Although it may seem to go in an opposite way as for the case of temperature variation, it is equivalent in nature. Indeed, the relaxation time increases when the pressure raises as seen on the inset (b) of Fig. (2). So an increase in pressure corresponds to an increase in the relaxation time and leads to vitrification if the pressure-rate-timescale is appropriate. When the pressure is decreased the relaxation time decreases and the system returns to the equilibrium after crossing the equilibrium line once.

This simple model gives us all the thermodynamic parameters of the system. It gives a qualitative behavior of the order parameter as a function of temperature variation and pressure variation. From the knowledge of the order parameter for any path in the $p - T$ plane, we shall compute the affinity and all the configurational contributions in the next section.

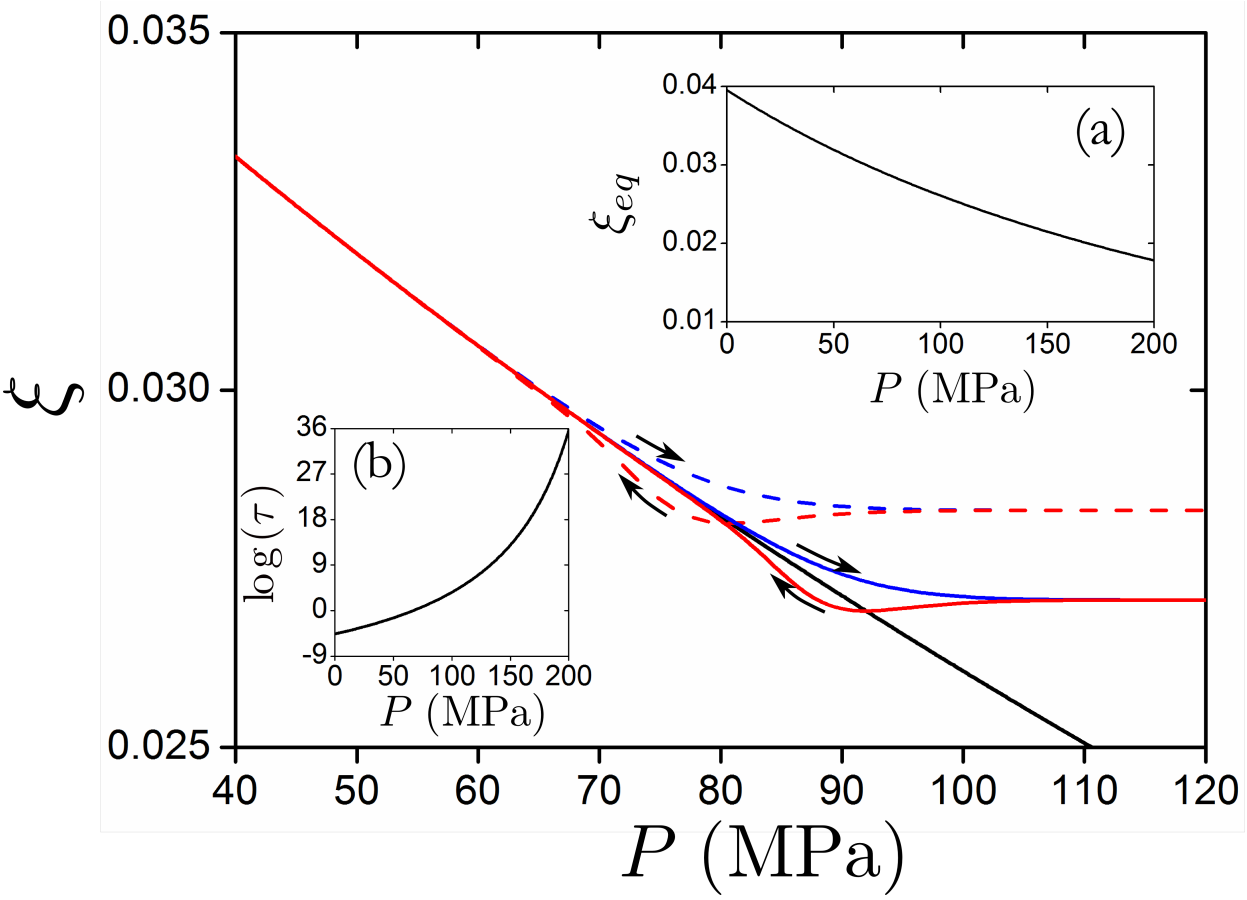

Figure 2: Evolution of the order parameter as a function of pressure at constant temperature $T = 271.6\,\mathrm{K}$. The arrows and colors indicate the sense of variation of the pressure : down and blue correspond to pressure increase and vitrification whereas up and red correspond to pressure decrease. The pressure variation rates are $\gamma_p = \pm 1.25$ MPa/min (thick lines) and $\gamma_T = \pm 25$ MPa/min (dashed lines). *Inset:* (a) Equilibrium order parameter as a function of pressure on the whole pressure range. (b) Evolution of $\log(\tau)$ as a function of pressure.

IV. DERIVATIVES OF THE AFFINITY AND EXPRESSION OF THE CONFIGURATIONAL PARTS

A. Affinity as a function of pressure and temperature

From the previous computations the values of the order parameter have been found as a function of temperature and pressure and as a function of the control parameter variations.

According to the out of equilibrium thermodynamics, the state of the system is entirely determined by the parameters T, p and ξ. We compute the affinity by using its definition (Eq. (3)). This gives:

$$A(T,p,\xi) = -\Delta E_0 - \frac{pV_0}{(1-\xi)^2} - RT\frac{ln\xi}{(1-\xi)^2} \tag{11}$$

The figure (3) and figure (4) show the plots of the affinity respectively as a function of T at a fixed pressure and as a function of p at a fixed temperature. The glass transition becomes observable when the affinity starts to deviate from zero. At temperatures and pressures in which the system is frozen and very little variations of the order parameter are observed, the affinity keeps varying linearly indicating that the variation of the control parameters pushes the system farher away from equilibrium without any influences of relaxational effects. During successive heating (or pressure decrease), the affinity undergoes a clear bump and even crosses the equilibrium $A = 0$ black line (or $\xi = \xi_{eq}$) before returning to equilibrium. Relaxational effects due to the unfreezing of structural degrees of freedom are important in these ranges. The variations of affinity clearly shows the out of equilibrium nature of the glass transition. They contribute significantly to the configurational parts of the thermodynamic coefficients as shown in the next paragraph.

B. Expression of the configurational parts general case

To evaluate the configurational parts of the thermodynamic coefficients, we need to evaluate the absolute derivative of the order parameter with respect to the control parameter that is in our case, either the temperature or the pressure. Since it is possible to compute the order parameter as shown in the preceding paragraphs, it is straightforward to evaluate the configurational contributions. Here, we focus on the affinity and express the total derivatives of the order parameter as a function of the affinity and its derivatives. This may prove to be useful in the general case when the expression of the Gibbs free energy is not known and when the out of equilibrium thermodynamic formalism is pushed to its limits [15].

Since the affinity is a state function, its total differential is :

$$dA = \left(\frac{\partial A}{\partial T}\right)_{p,\xi} dT + \left(\frac{\partial A}{\partial P}\right)_{T,\xi} dp + \left(\frac{\partial A}{\partial \xi}\right)_{p,T} d\xi \tag{12}$$

Maxwell relations [32] are used to transform the partial derivatives, and the equation above

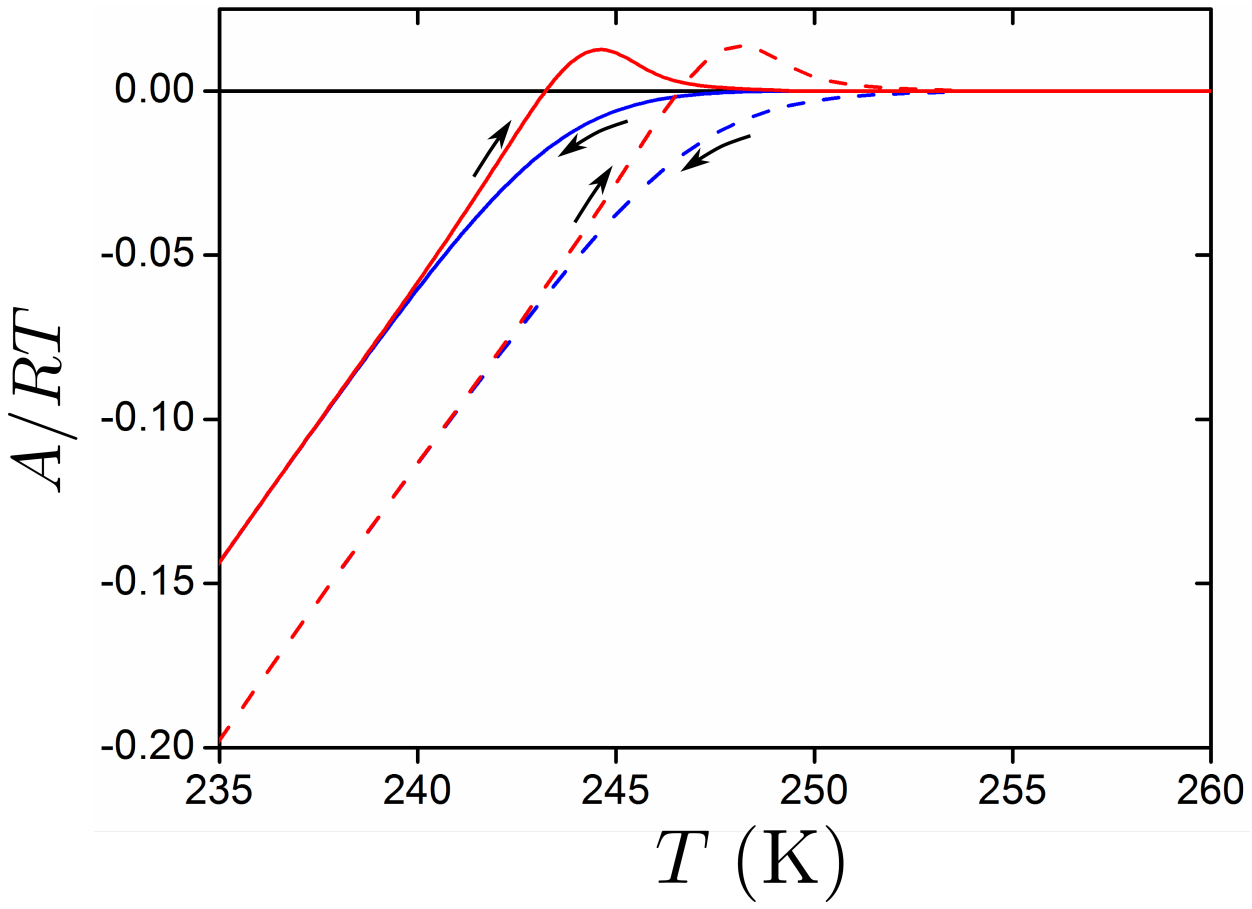

Figure 3: The affinity A divided by RT as function of temperature. The pressure is $p = 0.1$ MPa. The arrows and colors indicate the sense of variation of the temperature : down and blue correspond to cool down and vitrification whereas up and red correspond to reheating. The temperatures variation rates are $\gamma_T = \pm 0.3$ K/min (thick lines) and $\gamma_T = \pm 6$ K/min (dashed lines).

may be expressed in a practical way making explicitly apparent the infinitesimal time evolution :

$$\frac{dA}{dt} = \frac{\left[\left(\frac{\partial H}{\partial \xi}\right)_{p,T} + A\right]}{T}\frac{dT}{dt} - \left(\frac{\partial V}{\partial \xi}\right)_{T,p}\frac{dp}{dt} - \left(\frac{\partial^2 G}{\partial \xi^2}\right)_{p,T}\frac{d\xi}{dt} \tag{13}$$

The last term relates changes in affinity with changes of the order parameter (i.e relaxational effects due to structural changes). Irreversible thermodynamics requires that $\partial^2 G/\partial \xi^2|_{p,T} \geqslant 0$. All the thermodynamic coefficients which can be experimentally measured are calculated from this fundamental equation. We start with the configurational specific heat.

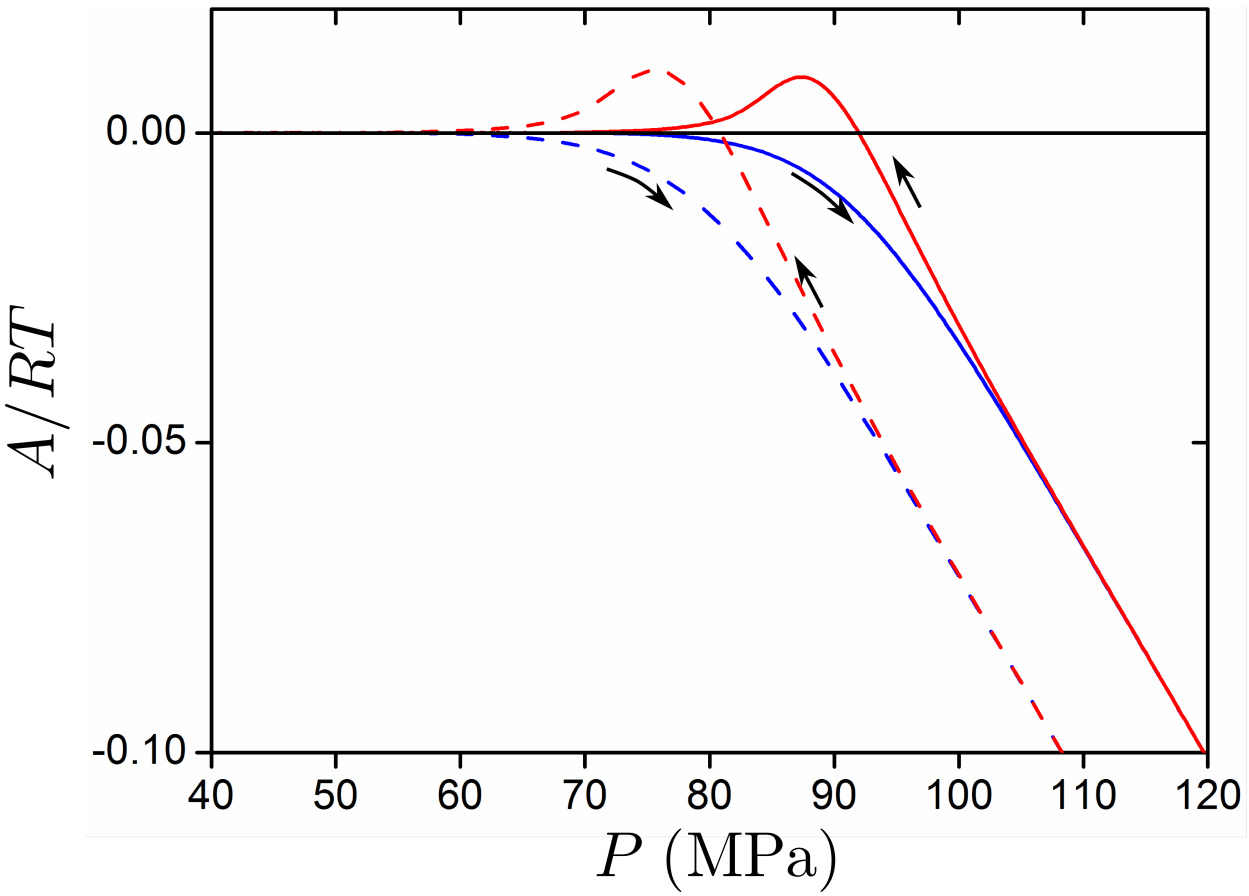

Figure 4: The affinity A divided by RT as a function of applied pressure. The temperature is $T = 271.6$ K. The arrows and colors indicate the sense of variation of the pressure : down and blue correspond to pressure increase and vitrification whereas up and red correspond to pressure decrease. The pressure variation rates are $\gamma_p = \pm 1.25$ MPa/min (thick lines) and $\gamma_T = \pm 25$ MPa/min (dashed lines)

C. Configurational specific heat

The isobaric heat capacity is measured experimentally by applying the following protocol. A certain amount of heat is exchanged reversibly between the system and an heat reservoir. This heat exchange occurs within a certain time scale, and the resulting temperature change is monitored on the same time scale. The pressure is kept constant during the measurement but the order parameter evolves freely according to Eq. (9). The heat capacity measured by the experimentalist is [32] :

$$C_p = \left(\frac{dH}{dT}\right)_p = \left(\frac{\partial H}{\partial T}\right)_{p,\xi} + \left(\frac{\partial H}{\partial \xi}\right)_{p,T}\left(\frac{d\xi}{dT}\right)_p = C_{p,\xi} + C_p^{\text{conf}} \tag{14}$$

The first term is written $\left(\frac{\partial H}{\partial T}\right)_{p,\xi} = C_{p,\xi}$. Since it implies a constant order parameter, it characterizes a frozen (glassy) state. The second term is the configurational heat capacity, which within the glass transition range is time dependent and equal to:

$$C_p^{\text{conf}}(t) = \left(\frac{\partial H}{\partial \xi}\right)_{p,T}\left(\frac{d\xi}{dT}\right)_p = \left(\frac{\partial H}{\partial \xi}\right)_{p,T}\left(\frac{d\xi/dt}{dT/dt}\right)_p \tag{15}$$

Owing to the fundamental equation (13), the configurational heat capacity is equal to:

$$C_p^{\text{conf}}(t) = \frac{\left(\frac{\partial H}{\partial \xi}\right)_{p,T}\left[\left(\frac{\partial H}{\partial \xi}\right)_{p,T} + A - T\left(\frac{dA}{dT}\right)_p\right]}{T\left(\frac{\partial^2 G}{\partial \xi^2}\right)_{p,T}} \tag{16}$$

This is the general expression of the isobaric configurational heat capacity of an out-of equilibrium system as a function of the partial derivatives involved in the process and particularly as a function of the affinity and its temperature derivative. This general expression has been used by one of us to derive the so-called expression of the frequency dependent complex heat capacity under linear regime assumption [33].

Following the same principle, other authors [18, 24] have derived these results basing their reasoning solely on the order parameter ξ. In extending their result to the affinity they conclude that the derivative of the affinity can be neglected in the equation (16) [24]. Their approximation is inconsistent since it implies that the affinity stays constant during the glass transition. Instead, Eq. (16) shows explicitly that the derivative of the affinity cannot be neglected compared with the other terms in the square bracket. Indeed, these three contributions are shown as a function of temperature for cooling and heating on Fig. (5). Neither during vitrification, nor during structural recovery the term $T\left(\frac{dA}{dT}\right)_p$ can be neglected with respect to the two others, $\left(\frac{\partial H}{\partial \xi}\right)_{p,T}$ and A.What can be neglected, however, is the affinity A as compared to $\left(\frac{\partial H}{\partial \xi}\right)_{p,T}$ within all the temperature range. This corresponds to the linearity assumption such as discussed in the appendix A of the reference [15].To further illustrate our point, the computations of the configurational specific heat are plotted on the figure (6) according to the results derived in Ref. [18, 23, 24] (see for example formula (17) of Ref. [18]) and compared with our results from Eq. (16). The qualitative behavior

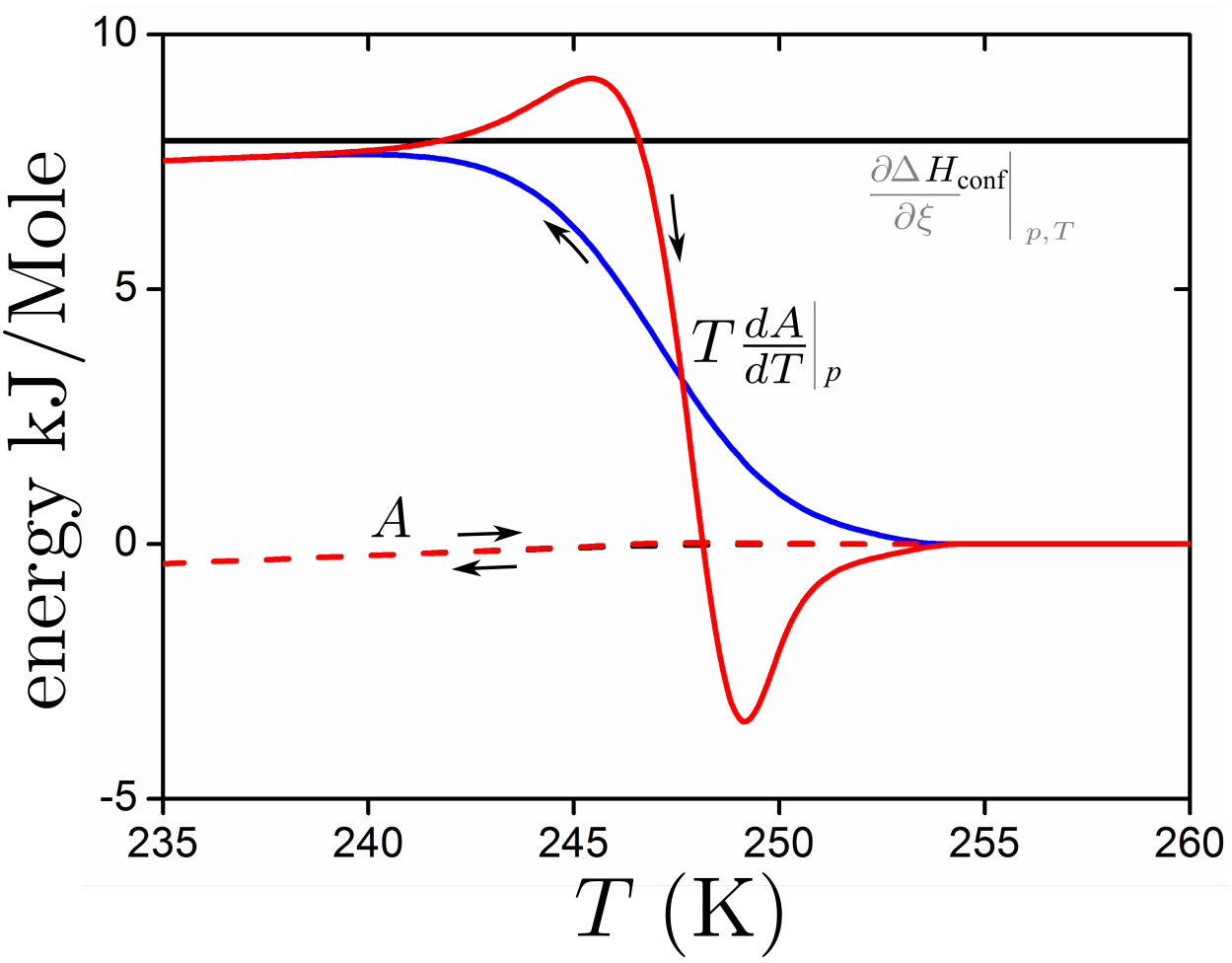

Figure 5: Comparison between the affinity A, its derivative with respect to temperature $T\left(\frac{dA}{dT}\right)_p$, and $\partial \Delta H_{conf}/\partial \xi)_{p,T}$ in a glass transition simulated for cooling and heating protocol of $\gamma_T = \pm 6\,\mathrm{K/min}$. The pressure is kept constant and equal to 0.1 MPa. The dashed line shows the affinity. Because of the scale, the cooling and heating curves are superimposed. The thick lines show TdA/dT and the arrows and colors indicate the sense of variation of the temperature : up and blue correspond to temperature decrease and vitrification whereas down and red correspond to subsequent reheating and structural recovery. Finally the constant black line corresponds to the term $\partial \Delta H_{conf}/\partial \xi)_{p,T}$.

of the specific heat computed using results of [18, 23, 24] is inconsistent with experimental data: no gradual decrease of the configurational specific heat is reproduced upon cooling, no overshoot of the specific heat is reproduced upon reheating, contrary to the behavior

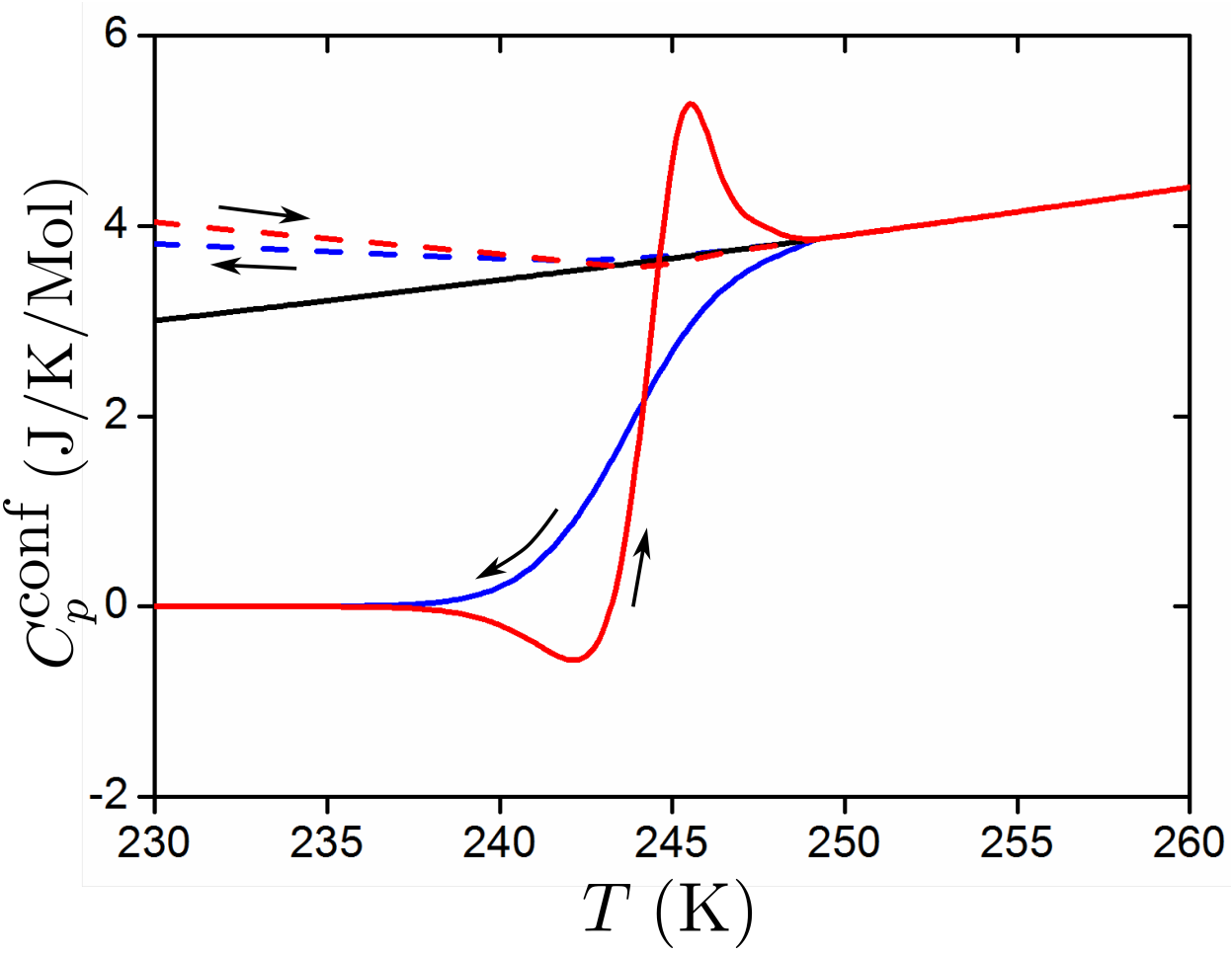

Figure 6: Computations of the configurational specific heat according to formula (17) of [18] (dashed lines) and Eq. (16) of this work (thick lines). The temperature variation rate is γ_T=±0.3 K/min. The pressure is kept constant and equal to 0.1 MPa. The arrows and colors indicate the sense of variation of the temperature : the blue color corresponds to temperature decrease and vitrification, whereas the red color corresponds to subsequent reheating and structural recovery. The equilibrium configurational specific heat is plotted as a thick black line (cooling or warming).

depicted from Eq. (16) by the blue and red thick lines.

The qualitative comparisons with experiments is best done by computing the normalized configurational specific heat [34, 35]: $C_p^N = (C_p^{\rm conf}/C_{p,eq}^{\rm conf})$. The Fig. (7) shows the results of the computations of the normalized configurational heat capacity for two different protocols. For the first protocol the temperature was ramped up and down at the same rate γ_T = ±0.3 K/min. Upon cooling the jump in the normalized configurational specific heat is the

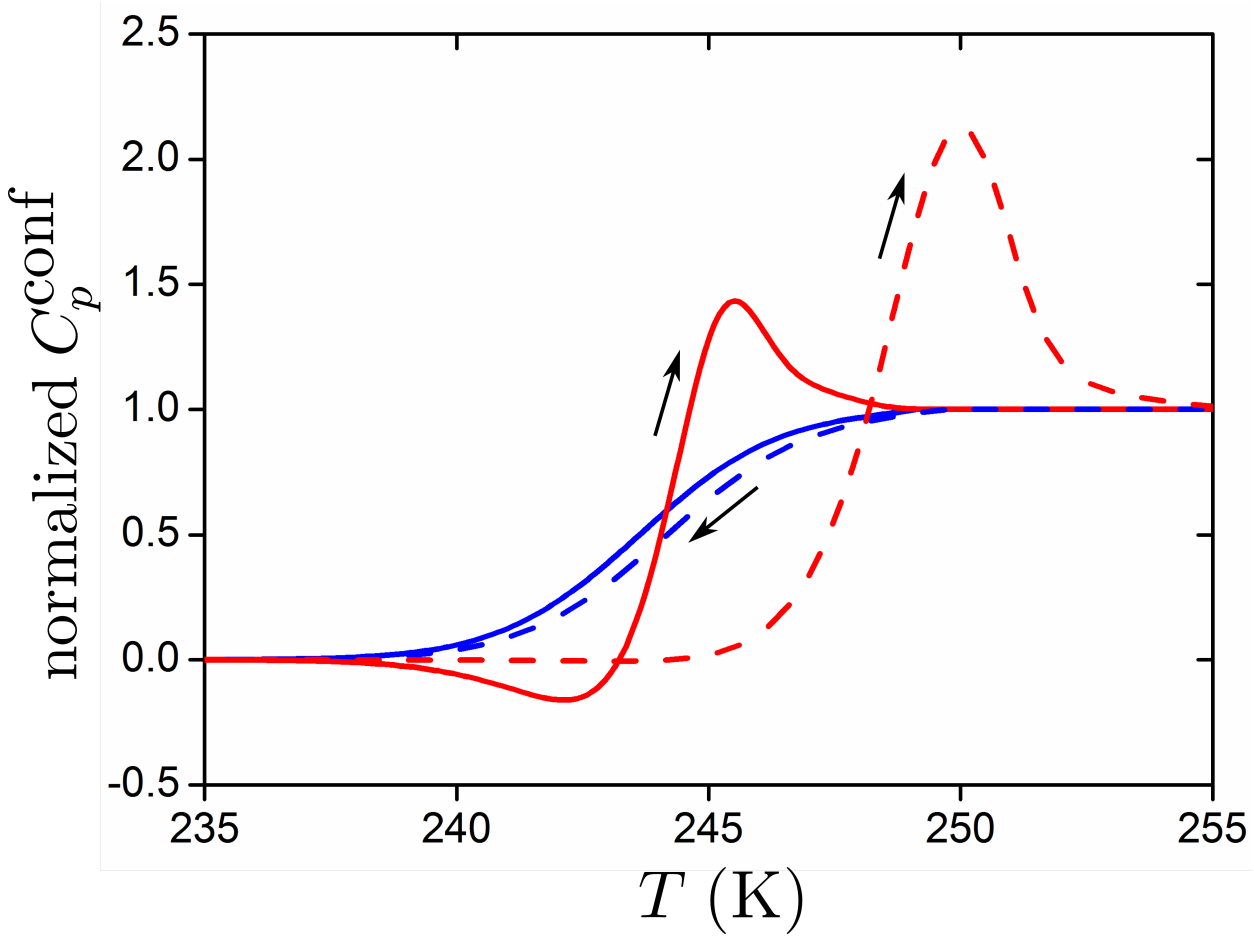

Figure 7: The normalized heat capacity at constant pressure ($p = 0.1$ MPa) as a function of temperature. The arrows and colors indicate the sense of variation of the temperature : down and blue correspond to temperature decrease and vitrification, whereas up and red correspond to subsequent reheating. The temperature variation rates are $\gamma_T = -0.3$ K/min (thick blue), $\gamma_T = +0.3$ K/min (thick red), $\gamma_T = -0.5$ K/min (dashed blue), $\gamma_T = +20$ K/min (dashed red).

signature of the glass transition and occurs in the same temperature range as the freezing of the order parameter (see Fig. (1)). Upon reheating at the same rate the glassy state disappears and the normalized specific heat first decreases and overshoots above the cooling curves. This overshoot in the heat capacity is characteristic of the structural recovery during reheating. It is commonly measured by differential scanning calorimetry.

For the second protocol, the rates of temperature variation were modified in order to assess their effects on the normalized specific heat, and to qualitatively compare the model

with experimental observations. A slight increase in the cooling rate ($\gamma_T = -0.5$ K/min) shows that the jump in the normalized specific heat occurs at a slightly higher temperature. This is coherent with experimental observations [36, 37]. An increase in the heating rate ($\gamma_T = 20$ K/min) strongly increases the overshoot of the normalized specific heat, as observed in experiments, and shifts it towards higher temperatures [36, 37]. It could also be remarked that, following the ratio of the cooling/heating temperature rates used, the model is able to reveal a decrease of the normalized heat capacity just before the overshoot. This effect, sometimes called "negative specific heat effect", is visible for the $\gamma_T = \pm 0.3$ K/min protocol while not accessible for the $\gamma_T = -0.5$ K/min and $\gamma_T = 20$ K/min protocol. This generally finer effect is also a typical characteristic of the glass transition [34, 38]. It results from a still decreasing enthalpy even during reheating.

Eventually, the model and computations are able to reproduce qualitatively the experimental behavior of the configurational specific heat. In the next sections we focus on the isobaric configurational coefficient of thermal expansion and isothermal compressibility.

D. Configurational coefficient of thermal expansion

The coefficient of thermal expansion is measured experimentally by applying the following protocol. Some heat is exchanged between the system and a heat reservoir within a given timescale. The pressure is kept constant but the volume, the temperature and the order parameter change. The coefficient of thermal expansion is obtained by computing the ratio:

$$\left(\frac{dV}{dT}\right)_p = V\alpha_p = \left(\frac{\partial V}{\partial T}\right)_{p,\xi} + \left(\frac{\partial V}{\partial \xi}\right)_{p,T}\left(\frac{d\xi}{dT}\right)_p$$

By using Maxwell relations [28, 32], the following expression for the configurational part of the dilatation coefficient is found :

$$\alpha_p^{\text{conf}} = \frac{1}{V}\left(\frac{\partial V}{\partial \xi}\right)_{p,T}\left(\frac{d\xi}{dT}\right)_p = \frac{\left(\frac{\partial V}{\partial \xi}\right)_{T,p}\left[\left(\frac{\partial H}{\partial \xi}\right)_{p,T} + A - T\left(\frac{dA}{dT}\right)_p\right]}{VT\left(\frac{\partial^2 G}{\partial \xi^2}\right)_{p,T}} \tag{17}$$

This last expression is the out of equilibrium thermodynamic expression of the configurational isobaric dilatation coefficient emphasizing the role of the affinity. This expression makes explicit use of the affinity, its temperature derivative, and coefficients such as $\left(\frac{\partial V}{\partial \xi}\right)_{T,p}$,

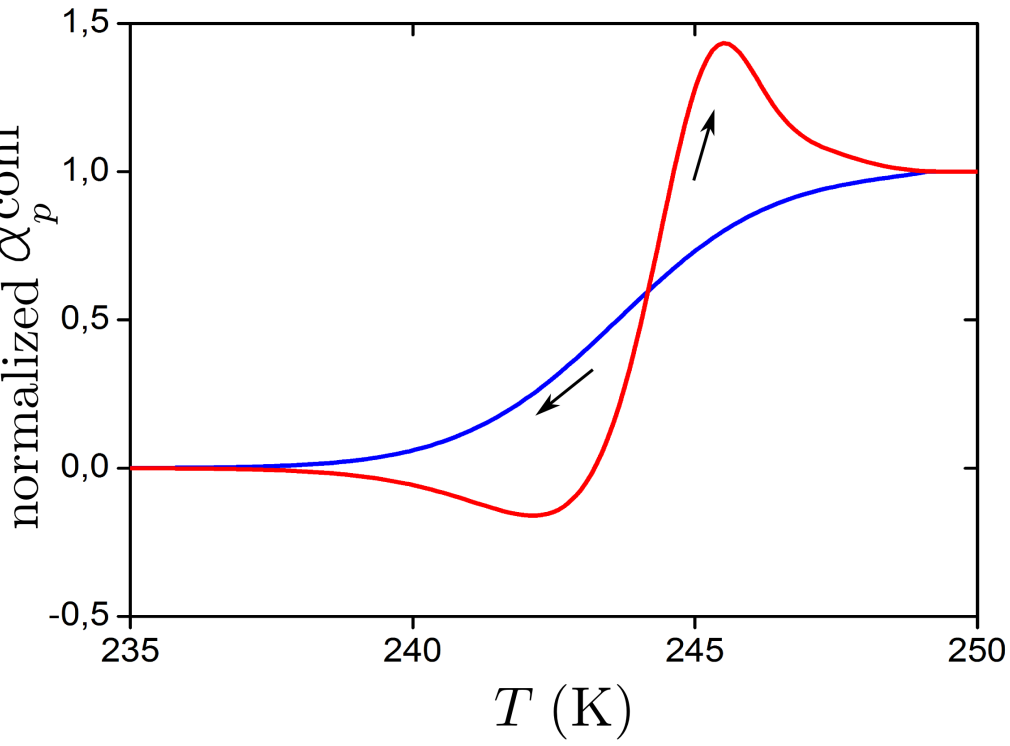

Figure 8: Computation of the normalized configurational coefficient of thermal expansion. The temperature variation rate is γ_T=±0.3 K/min. The pressure is kept constant and equal to 0.1 MPa. The arrows and colors indicate the sense of variation of the temperature : the blue color corresponds to temperature decrease and vitrification, whereas the red color corresponds to subsequent reheating and structural recovery.

$\left(\frac{\partial H}{\partial \xi}\right)_{p,T}$, $\left(\frac{\partial^2 G}{\partial \xi^2}\right)_{p,T}$ as well as the volume and temperature. As for the normalized heat capacity, the normalized coefficient of thermal expansion, $\alpha_p^N = \alpha_p^{\rm conf}/\alpha_{p,eq}^{\rm conf}$is plotted on Fig. (8), as a function of temperature during a cooling and successive heating at a rate of $\gamma_T = \pm 6\,$K/min. The pressure is constant and equal to 0.1 MPa. As it can be also shown from equations, exactly the same curves are obtained as for the normalized isobaric heat capacity [39, 40].

E. Configurational compressibility

We consider here the isothermal compressibility. It is measured experimentally by using the following protocol. The external pressure is varied with a given timescale and the resulting volume change is recorded on the same time scale. The temperature is kept constant and the order parameter evolves according to Eq. (9). The isothermal compressibility is obtained by computing the following ratio :

$$-V\kappa_T = \left(\frac{dV}{dp}\right)_T = \left(\frac{\partial V}{\partial p}\right)_{T,\xi} + \left(\frac{\partial V}{\partial \xi}\right)_{T,p}\left(\frac{d\xi}{dp}\right)_T$$

By applying the same reasoning as in the previous parts the configurational isothermal compressibility is expressed as :

$$\kappa_T^{\text{conf}} = -\frac{1}{V}\left(\frac{\partial V}{\partial \xi}\right)_{T,p}\left(\frac{d\xi}{dp}\right)_T = \frac{\left(\frac{\partial V}{\partial \xi}\right)_{T,p}\left[\left(\frac{\partial V}{\partial \xi}\right)_{T,p} + \left(\frac{dA}{dp}\right)_T\right]}{V\left(\frac{\partial^2 G}{\partial \xi^2}\right)_{p,T}} \tag{18}$$

As previously, this expression emphasizes the role of the affinity derivative, but this time with respect to pressure. In order to evaluate the importance of the terms in the bracket, $-\left(\frac{\partial V}{\partial \xi}\right)_{T,p}$ and $\left(\frac{dA}{dp}\right)_T$ are plotted on Fig.(9) for two different rates of pressure variation at constant temperature (see legend for details). Both contribute significantly to the configurational isothermal compressibility, and the affinity derivative can not be neglected [24]. On this figure it is observed that above 100 MPathe two terms are approximately equivalent in absolute value.

In a similar way to what has been done for the configurational specific heat and configurational dilatation coefficient, we define the normalized configurational compressibility as the ratio of the configurational compressibility and the equilibrium configurational compressibility: $\kappa_T^N = \kappa_T^{\text{conf}}/\kappa_{T,eq}^{\text{conf}}$. This ratio is represented on Fig. (10) for two pressure variation rates of 1.5 MPa/min and of 25 MPa/min. Vitrification by pressure increase is clearly evidenced, and the higher the pressure rate is, the lower the glass transition pressure is. The two protocols have been carried out for a constant temperature of 271.6 K. It may be shown that the characteristic pressure around which the vitrification process occur is directly dependent on temperature, and the highest the constant temperature is, the lowest the glass transition pressure is, for a given pressure rate.

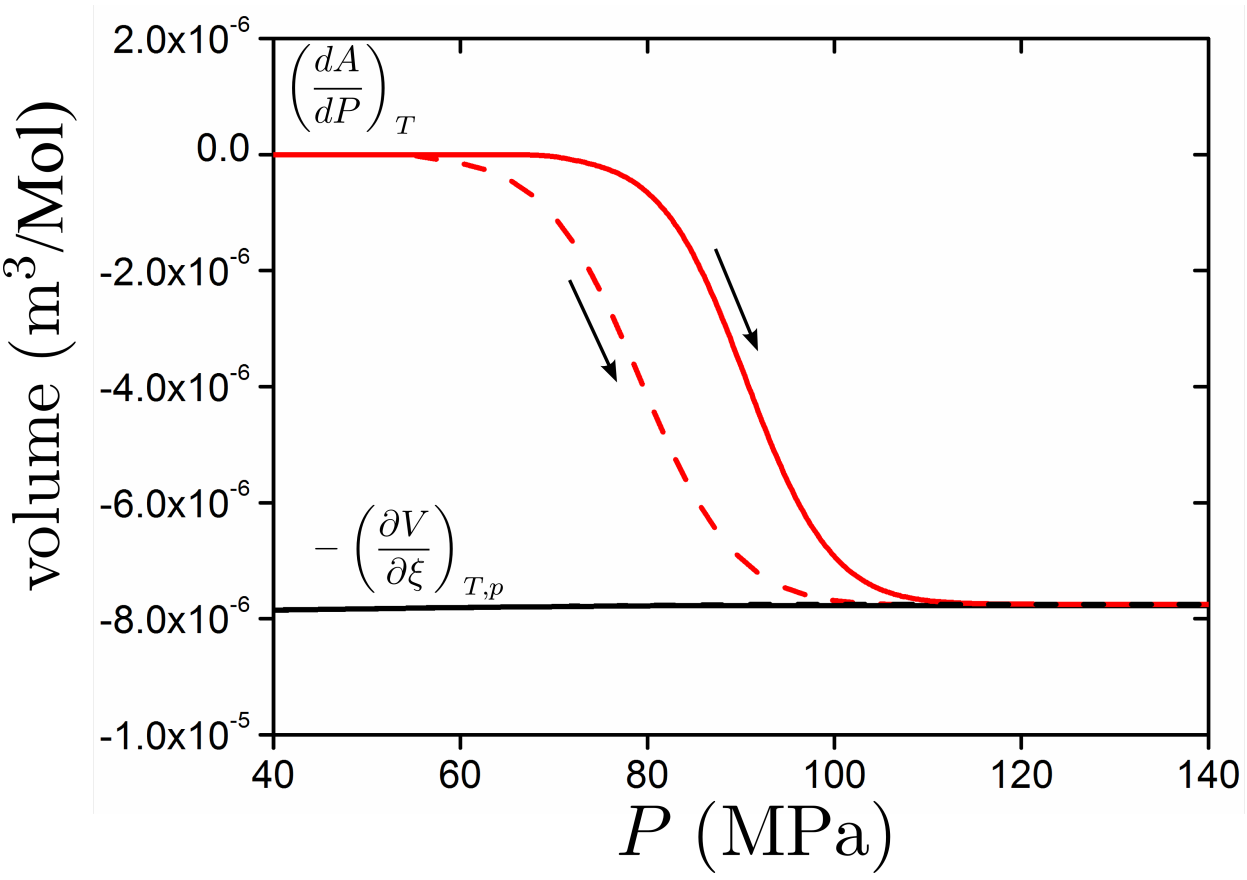

Figure 9: Comparison of $\left(\frac{dA}{dp}\right)_T$ (red lines) and $-\left(\frac{\partial V}{\partial \xi}\right)_{T,p}$ (black lines) for two pressure rates. The arrows indicate the sense of pressure variation. The pressure variation rates are $\gamma_P = 1.5$ MPa/min (thick line) and $\gamma_P = 25$ MPa/min (dashed line).

V. FICTIVE TEMPERATURE

Tool defined the fictive temperature T_f as the effective temperature of the configurational degrees of freedom in a glass-former [41, 42]. By definition, the configurational enthalpy, δH_{conf}, of the non-equilibrium glassy state at the temperature T, equals that of the corresponding equilibrium liquid taken at the fictive temperature:

$$\delta H_{conf}(T) = \delta H^{eq}_{conf}(T_f) \tag{19}$$

From this definition, in deriving with respect to temperature this gives directly the configurational heat capacity [38, 43]:

$$C_p^{\text{conf}}(T) = C_{p,eq}^{\text{conf}}(T_f)\frac{dT_f}{dT} \tag{20}$$

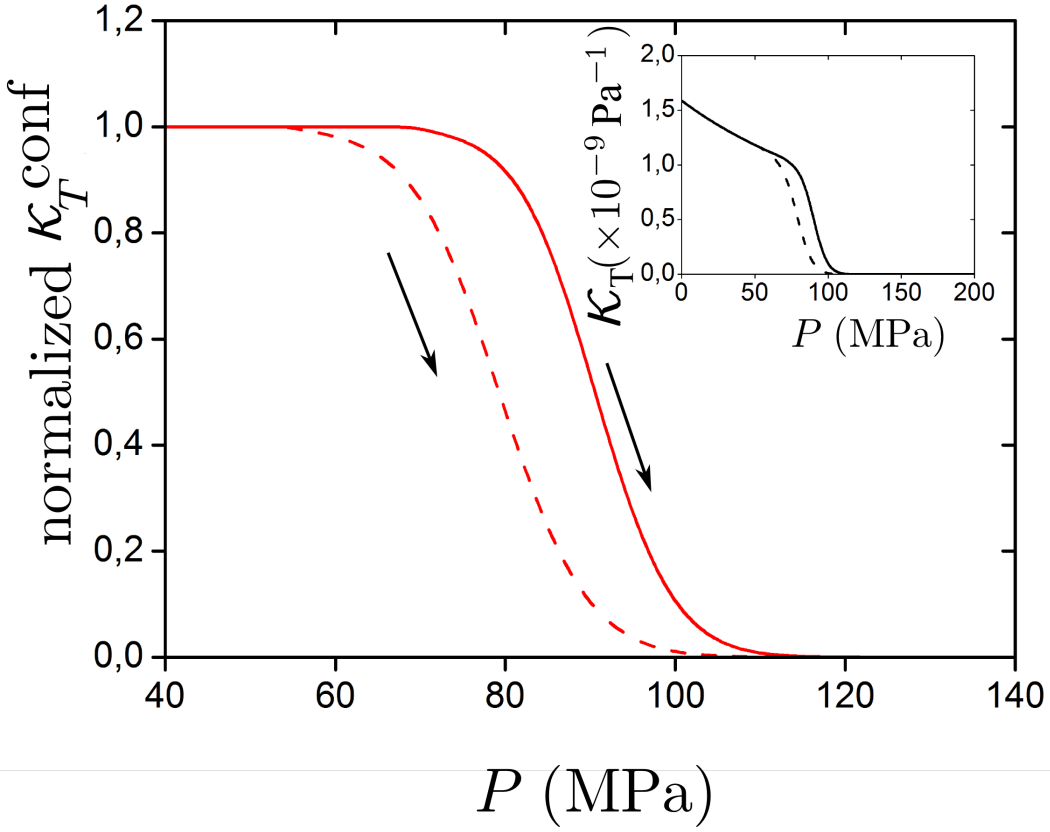

Figure 10: Normalized configurational compressibility at constant temperature of 271.6 K. The data for a pressure variation rate of $\gamma_p = 1.5$ MPa/min (thick line) and of $\gamma_p = 25$ MPa/min (dashed line) are represented. *Inset* : absolute values of the configurational compressibility over the full pressure range for $\gamma_p = 1.5$ MPa/min (thick line) and $\gamma_p = 25$ MPa/min (dashed line).

So, the normalized heat capacity (Cf. for example curves on Fig. (7)), is equivalent to the temperature derivative of the fictive temperature:

$$C_p^N = \frac{dT_f}{dT} \tag{21}$$

This latter equality can therefore be used to obtain directly the fictive temperature by integration of the normalized heat capacity curves. The result of such integration, for a simple cooling rate protocol with $\gamma = -0.5$ K/min, is plotted on Fig. (11) as the thick red line.

In the reference [22] and [24], Schmelzer, Tropin, and co-workers proposed a model-independent definition of the fictive temperature (and fictive pressure) based on the classical thermodynamic definition of a temperature:

$$T_f = \left(\frac{\partial U}{\partial S}\right)_V \tag{22}$$

or equivalently at constant pressure,

$$T_f = \left(\frac{\partial H}{\partial S}\right)_p \tag{23}$$

The difference with usual temperatures comes here from the presence of the term $Ad\xi$ (or $\sum_i A_i d\xi_i$ for multi order-parameters, see [24]) in the expression of the first law of thermodynamics as defined in De Donder's thermodynamics:

$$dH = TdS + Vdp - Ad\xi \tag{24}$$

In developing $d\xi$ as a function of the variables S, p and A, this yields to:

$$dH = \left(T - A\left(\frac{\partial \xi}{\partial S}\right)_{p,A}\right) dS + \left(V - A\left(\frac{\partial \xi}{\partial p}\right)_{S,A}\right) dp - A\left(\frac{\partial \xi}{\partial A}\right)_{p,S} dA \tag{25}$$

The third term is absent in references [22, 24]. Therefore, for the sake of preciseness, the definition proposed by Schmelzer and co-workers is not only defined as the entropy derivative of the internal energy (constant volume) or entropy derivative of the enthalpy (constant pressure), but also as partial derivative at constant affinity. For example, at constant pressure this yields to:

$$T_f = \left(\frac{\partial H}{\partial S}\right)_{p,A} = T - A\left(\frac{\partial \xi}{\partial S}\right)_{p,A} \tag{26}$$

or $T_f = \left(\frac{\partial U}{\partial S}\right)_{V,A} = T - A\left(\frac{\partial \xi}{\partial S}\right)_{V,A}$ at constant volume and affinity (see Eq. (48) in Ref. [22], or Eq. (44) in Ref. [24]). By contrast in Eq. (24), it is observed that the usual temperature of the system is rather defined as entropy derivative at constant order parameter. For example, at constant pressure:

$$T = \left(\frac{\partial H}{\partial S}\right)_{p,\xi} \tag{27}$$

or $T = \left(\frac{\partial U}{\partial S}\right)_{V,\xi}$ at constant volume. It is worth noting that under this definition, the fictive temperature may be a partial derivative at constant affinity while the usual temperature is a partial derivative at constant order parameter.

We shall show here whether this thermodynamic-like definition of the fictive temperature has something in common with the classical definition of the fictive temperature such as proposed by Tool and discussed previously. Firstly, it has to be mentioned that in references [22, 24], the following underlying assumption is used: the partial derivative $\left(\frac{\partial \xi}{\partial S}\right)_{p,A}$ has to be equivalent to $\left(\frac{\partial \xi}{\partial S}\right)_{p,T}$ (or if volume is constant, we must have the equality between $\left(\frac{\partial \xi}{\partial S}\right)_{V,A}$ and $\left(\frac{\partial \xi}{\partial S}\right)_{V,T}$). This is, as it follows from cited papers, however, not the original intention of mentioned authors because terms containing the affinity variation in the total differential of U or H have been neglected. It turns out that, under this assumption, the entropy of mixing coming from the hole theory can be used, $\left(\frac{\partial \xi}{\partial S}\right)_{p,T} = 1/\left[R\left[\ln(1-\xi) + \frac{\xi}{1-\xi}\ln\xi\right]\right]$, in order to calculate T_f from Eq. (26). The fictive temperature following the equation (26) can also be written as a function of A and $\left(\frac{\partial H}{\partial \xi}\right)_{p,T}$ by using the thermodynamic equality $T\left(\frac{\partial S}{\partial \xi}\right)_{p,T} = A + \left(\frac{\partial H}{\partial \xi}\right)_{p,T}$:

$$T_f = T - A\left(\frac{\partial \xi}{\partial S}\right)_{p,T} = T\left[1 - \frac{A}{\left[A + \left(\frac{\partial H}{\partial \xi}\right)_{p,T}\right]}\right] \tag{28}$$

The temperature behavior of this fictive temperature is plotted on the figure (11) as the thick blue line following the same cooling rate protocol of -0.3 K/min. The agreement of the two curves coming from the two definitions above is of very high quality. On the same figure, we represent the fictive temperature calculated by Tropin *et al.* as the thick black line on Fig. (11)). The fictive temperature increasing at low temperatures such as depicted on Fig. (4) of Ref. [24], is inconsistent with frozen-in fictive temperatures in the glassy state. This is due to an approximated expression taken by the authors of the cited papers for the affinity, $A \simeq -RT\left(\frac{\xi - \xi_{eq}}{\xi_{eq}}\right)$ (see for example Eq. (50) of Ref. [22]), which is valid only under particular conditions.

In conclusion, the model-independent definition of the fictive temperature given by Schmelzer and co-workers is consistent with the classical (or Tool's definition) of the fictive temperature, only if the fundamental assumption that $\left(\frac{\partial \xi}{\partial S}\right)_{p,A}$ is equivalent to $\left(\frac{\partial \xi}{\partial S}\right)_{p,T}$ is valid. This underlying assumption seems exact upon the framework of the lattice-hole model, but may not be true in general. Consequently, despite its interest and simplicity, the new definition proposed across Eq. (26) for example, is not a model independent thermodynamic-like definitions of the fictive temperature. Some of the authors of the present

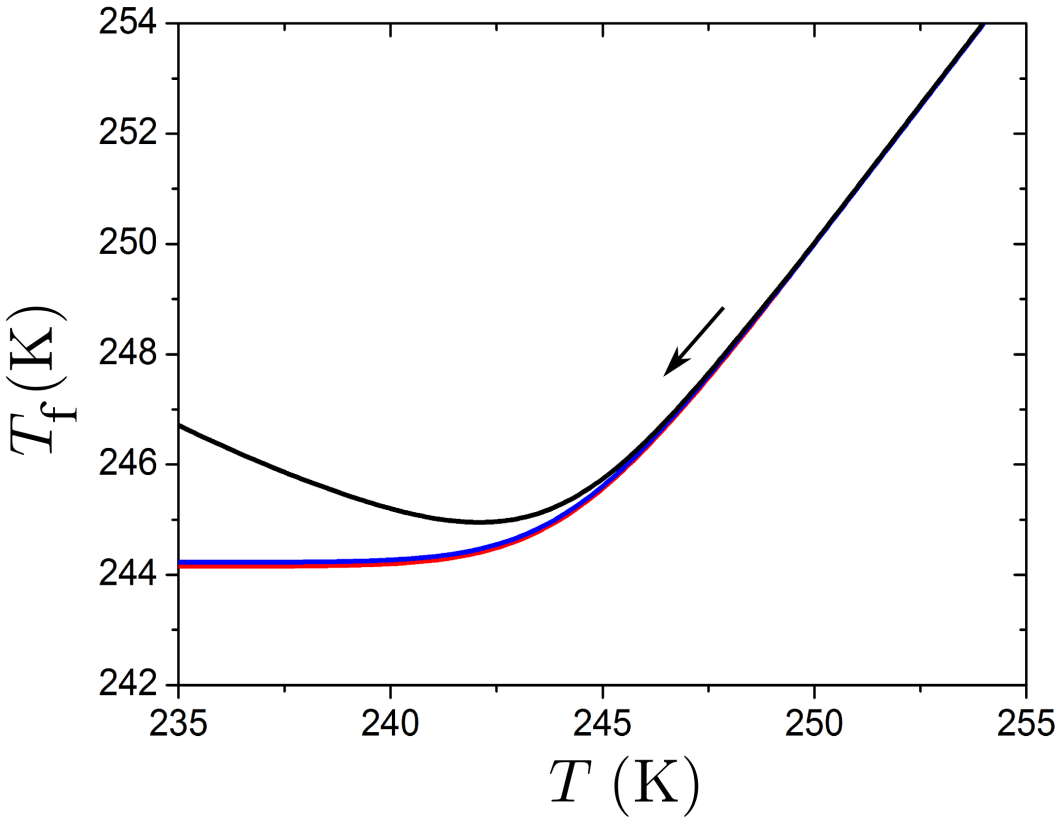

Figure 11: Fictive temperatures as a function of temperature during cooling at a temperature rate of -0.5 K/min at constant pressure of 0.1MPa. The read one, which comes from the classical definition of the fictive temperature, is issued from integration of the corresponding normalized heat capacity data. The blue one is issued from the Eq. (28). The black one is inferred from calculation of Tropin and co-workers with an approximate value of the affinity (see Eq. (50) of Ref. [22]).

work have given a thermodynamic-like definition of the fictive temperature based on the notion of entropy production, which is present in any irreversible processes, not only the glass transition process [13]. Although we do not discuss it here, exactly the same arguments can be given for the definition of the fictive pressure proposed in Ref. [22, 24].

VI. CONCLUSION AND PERSPECTIVES

We have presented a minimalist model (the lattice-hole model of liquids) which, if the laws of non-equilibrium thermodynamics are rigorously applied, is able to reproduce qualitatively the characteristic behavior of thermodynamic coefficients such as C_p, α_p or κ_T during a glass transition. The characteristic features of vitrification and structural recovery obtained under different conditions, particularly upon temperature or pressure perturbations, have been reproduced. The possibility to calculate jumps in C_p, α_p or κ_T at T_g or p_g following different simulated experimental protocols have practical applications and allows one to define and compute classical Prigogine-Defay ratio as well as linear PD ratio [44] or non-equilibrium Prigogine-Defay ratio [15].

While the model is able to reveal most of the principal characteristics of the glass transition, it describes also qualitatively some experimental behavior. For example, the predicted glass transition temperature of *o*-terphenyl is quantitatively consistent with experiments. On the other hand, using the model *ad hoc* to fit experimental data for C_p, α_p or κ_T such as for example done with TNM model, or Adam-Gibbs approach, has not yet been performed, and it is not the purpose of this work. Instead, we focused on the role of pressure and affinity. If data are to be fitted according to the model, it may require the addition of new ingredients such as, among others:

i) coexistence of several order parameters [3].

ii) deviation from the linear regime.

iii) dependence of the relaxation time on the non-equilibrium state of the system [35, 45].

iv) effect of heterogeneities and the presence of a distribution of relaxation times [35, 45].

As an example of the limit of the model, in its current shape, it is not able to reveal the apparition of the Kovacs effect after cross-over experiments such as studied recently [16, 17]. Promising works by A. Lion and co-workers who developed for few years a more accurate non-equilibrium thermodynamics with internal state variables offer interesting perspectives in this direction. [10–12].

---

[1] T. D. Donder and P. V. Rysselberghe, *Thermodynamic theory of Affinity, a Book of Principles* (Standford University press, 1936).

[2] I. Prigogine and R. Defay, *Chemical Thermodynamics* (Longmans, 1954).

[3] R. O. Davies and G. O. Jones, Advanc. Phys. (Phil. Mag. Suppl.) **2**, 370 (1953).

[4] X. Guo, M. Potuzak, J. C. Mauro, D. C. Allan, T. J. Kiczenski, and Y. Yue, J. Non-Cryst. Solids **357**, 3230 (2011).

[5] R. J. A. J. C. Mauro, J. Am. Ceram. Soc. **93**, 1026 (2010).

[6] P. D. Gujrati, Phys. Rev. E **81**, 051130 (2010).

[7] E. Bouchbinder and J. S. Langer, Phys. Rev. E **80**, 031131 (2009).

[8] E. Bouchbinder and J. S. Langer, Phys. Rev. E **80**, 031132 (2009).

[9] H. Kobayashi and H. Takahashi, J. Chem. Phys. **132**, 104504 (2010).

[10] A. Lion and B. Yagimili, Thermochim. Acta **490**, 64 (2009).

[11] A. Lion, C. Liebl, S. Kolmeder, and J. Peters, J. Mech. Phys. Solids **58**, 1338 (2010).

[12] A. Lion, J. Peters, and S. Kolmeder, Thermochim. Acta **522**, 182 (2011).

[13] J.-L. Garden, J. Richard, and H. Guillou, J. Chem. Phys. **129**, 044508 (2008).

[14] K. Mrabet, R. Rahouadj, and C. Cunat, Polym. Engineering Sc. **45**, 42 (2005).

[15] J.-L. Garden, H. Guillou, J. Richard, and L. Wondraczek, J. Non-equi. Therm. **accepted** (2012).

[16] E. Bouchbinder and J. S. Langer, Soft Matter **6**, 3065 (2010).

[17] F. Mossa and F. Sciortino, Phys. Rev. Lett. **92**, 045504 (2004).

[18] J. W. P. Schmelzer and I. Gutzow, J. Chem. Phys. **125**, 184511 (2006).

[19] J. Möller, I. Gutzow, and J. W. P. Schmelzer, J. Chem. Phys. **125**, 094505 (2006).

[20] I. Gutzow, J. W. P. Schmelzer, and B. Petroff, J. of Engineer. Thermo. **16**, 205 (2007).

[21] I. Gutzow, J. W. P. Schmelzer, and B. Petroff, J. Non-Cryst. Solids **354**, 311 (2008).

[22] J. W. P. Schmelzer and I. Gutzow, J. Non-Cryst. Solids **355**, 653 (2009).

[23] T. V. Tropin, J. W. P. Schmelzer, and C. Schick, J. Non-Cryst. Solids **357**, 1291 (2011).

[24] T. V. Tropin, J. W. P. Schmelzer, and C. Schick, J. Non-Cryst. Solids **357**, 1303 (2011).

[25] B. Wunderlich, D. M. Bodily, and M. H. Kaplan, J. Appl. Phys. **35**, 95 (1964).

[26] T. Somcynsky and R. simha, J. Appl. Phys. **42**, 4545 (1971).

[27] J. Frenkel, *Kinetic Theory of Liquids* (Dover, 1955).

[28] I. Gutzow and J. Schmelzer, *The Vitreous State* (1995).

[29] N. Hirai and H. Eyring, J. Appl. Phys. **29**, 810 (1958).

[30] M. Naoki and S. Koeda, J. Phys. Chem. **93**, 948 (1989).

[31] H. Leyser, A. Schulte, W. Doster, and W. Petry, Phys. Rev. E **51**, 5899 (1995).

[32] I. Prigogine and R. Defay, *Thermodynamique Chimique (Nouvelle rédaction)* (1950).

[33] J.-L. Garden, Thermochim. Acta **452**, 85 (2007).

[34] C. T. Moynihan, P. B. Macedo, C. J. Montrose, P. K. Gupta, M. A. DeBolt, J. F. Dill, B. E. Dom, P. W. Drake, A. J. Easteal, P. B. Elterman, et al., A. N. Y. Acad. Sci. **15**, 15 (1976).

[35] I. M. Hodge, J. Non-Cryst. Solids **169**, 211 (1994).

[36] R. Svoboda, P. Pustkova, and J. Malek, J. Phys. Chem. Solids **68**, 850 (2007).

[37] R. Svoboda, P. Pustkova, and J. Malek, Polymer **49**, 3176 (2008).

[38] M. A. DeBolt, A. J. Easteal, P. B. Macedo, and C. T. Moynihan, J. Am. Ceram. Soc. **59**, 16 (1976).

[39] J. M. Hutchinson, M. Ruddy, and M. R. Wilson, Polymer **29**, 152 (1988).

[40] J. Gottsmann, D. B. Dingwell, and C. Gennaro, American Mineralogist **84**, 1176 (1999).

[41] A. Q. Tool, J. res. Natl. Bur. Stand. **34**, 199 (1945).

[42] A. Q. Tool, J. Am. Ceram. Soc. **29**, 240 (1946).

[43] C. T. Moynihan, A. J. Easteal, M. A. DeBolt, and J. Tucker, J. Am. Ceram. Soc. **59**, 12 (1976).

[44] D. Gundermann, U. R. Pedersen, T. Hecksher, N. P. Bailey, B. Jakobsen, T. Christensen, N. B. Olsen, T. B. Schrøder, D. Fragiadakis, R. Casalini, et al., Nature Phys. **7**, 816 (2011).

[45] G. B. McKenna and C. A. Angell, J. Non-Cryst. Solids **131-133**, 528 (1991).

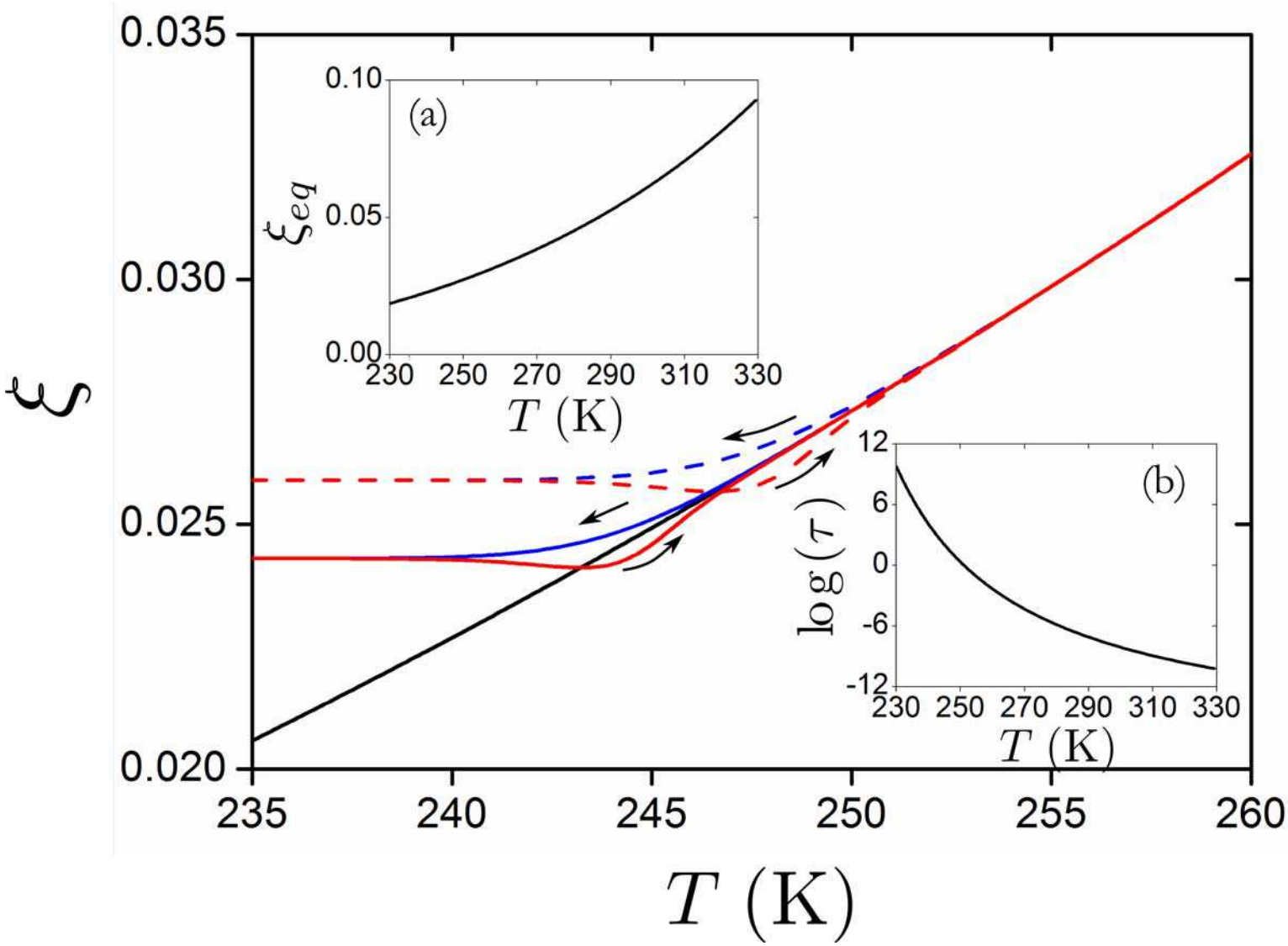
0.035
0.030
0.025
0.020
235
240
245
250
255
260
ξ
T (K)
(a)
0.10
0.05
0.00
ξ_{eq}
230 250 270 290 310 330
T (K)
(b)
12
6
0
-6
-12
log(τ)
230 250 270 290 310 330
T (K)

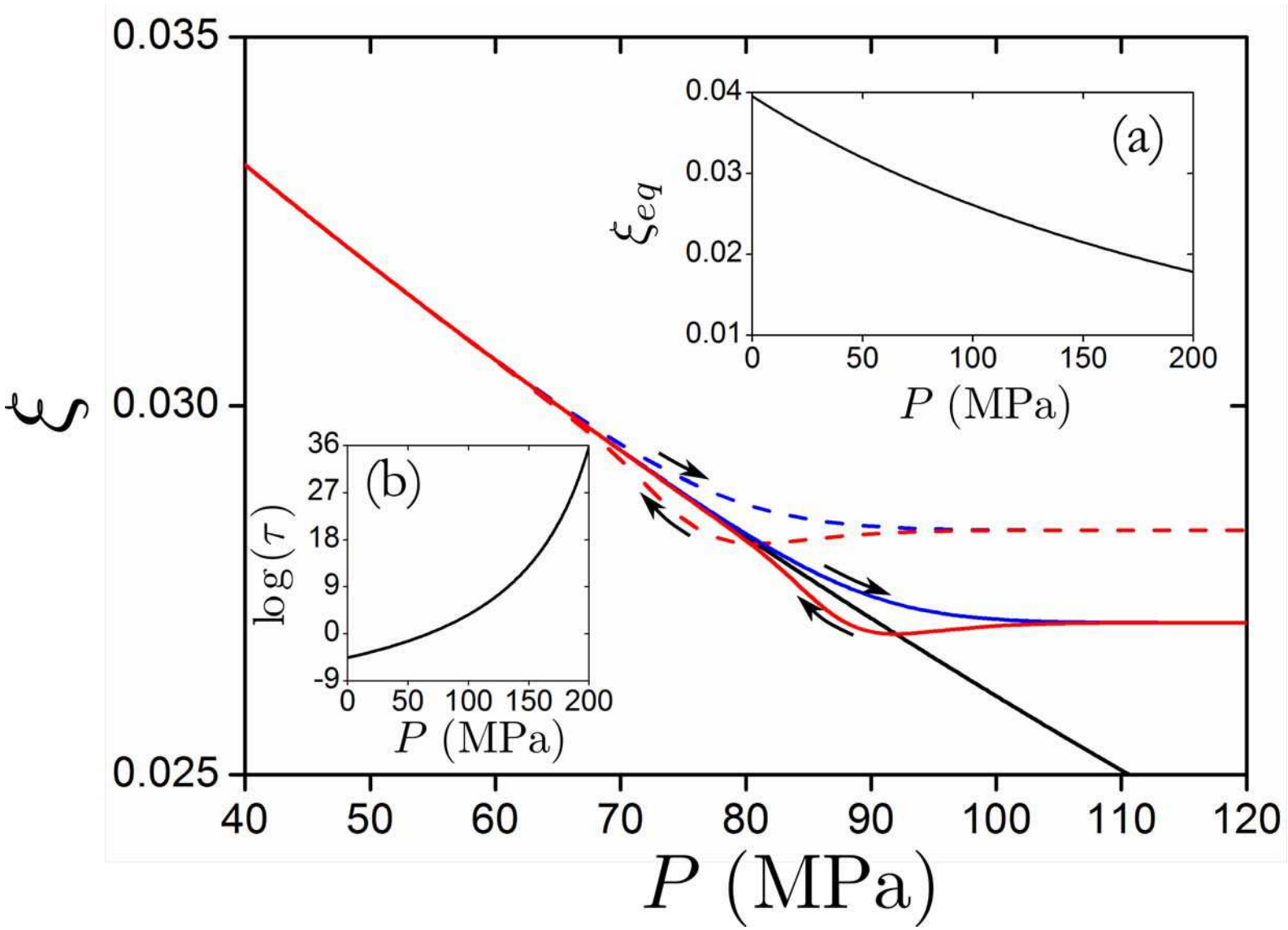
0.035
0.030
0.025
ξ
40
50
60
70
80
90
100
110
120
P (MPa)
0.04
0.03
0.02
0.01
ξ_{eq}
(a)
0
50
100
150
200
P (MPa)
36
27
18
9
0
-9
$\log(\tau)$
(b)
0
50
100
150
200
P (MPa)

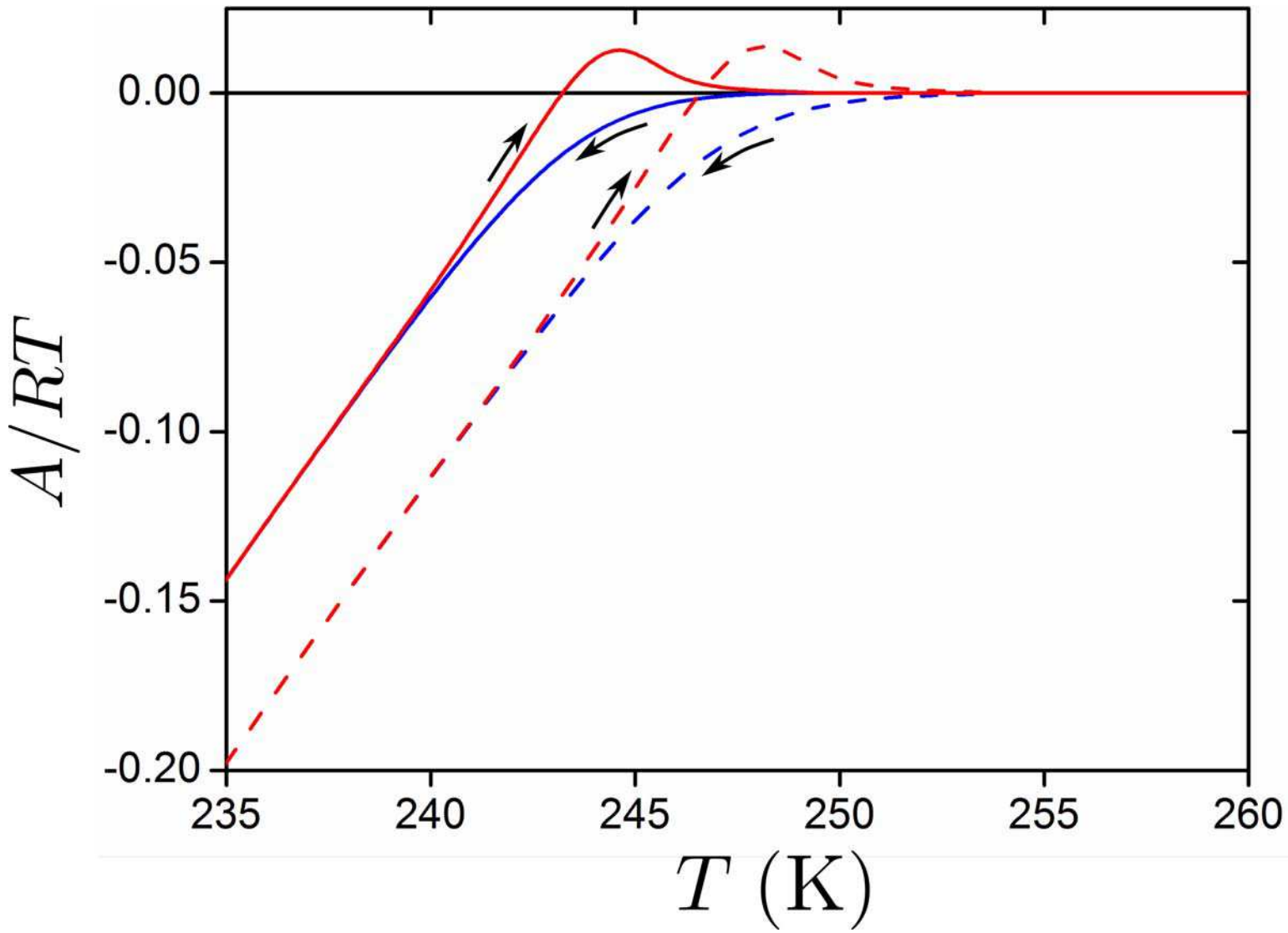
0.00
-0.05
-0.10
-0.15
-0.20
A/RT
235
240
245
250
255
260
T (K)

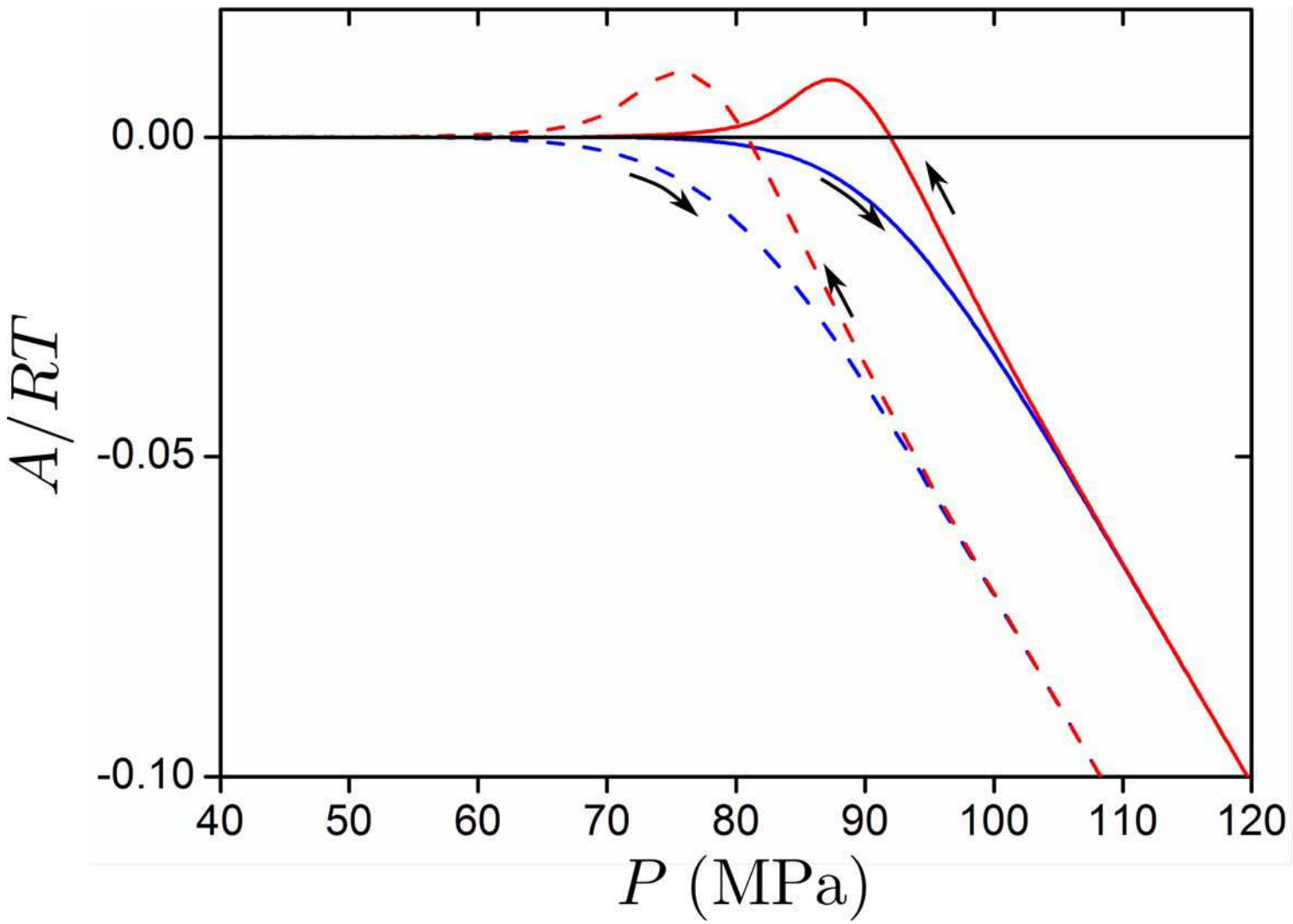
0.00
-0.05
-0.10
40
50
60
70
80
90
100
110
120
A/RT
P (MPa)

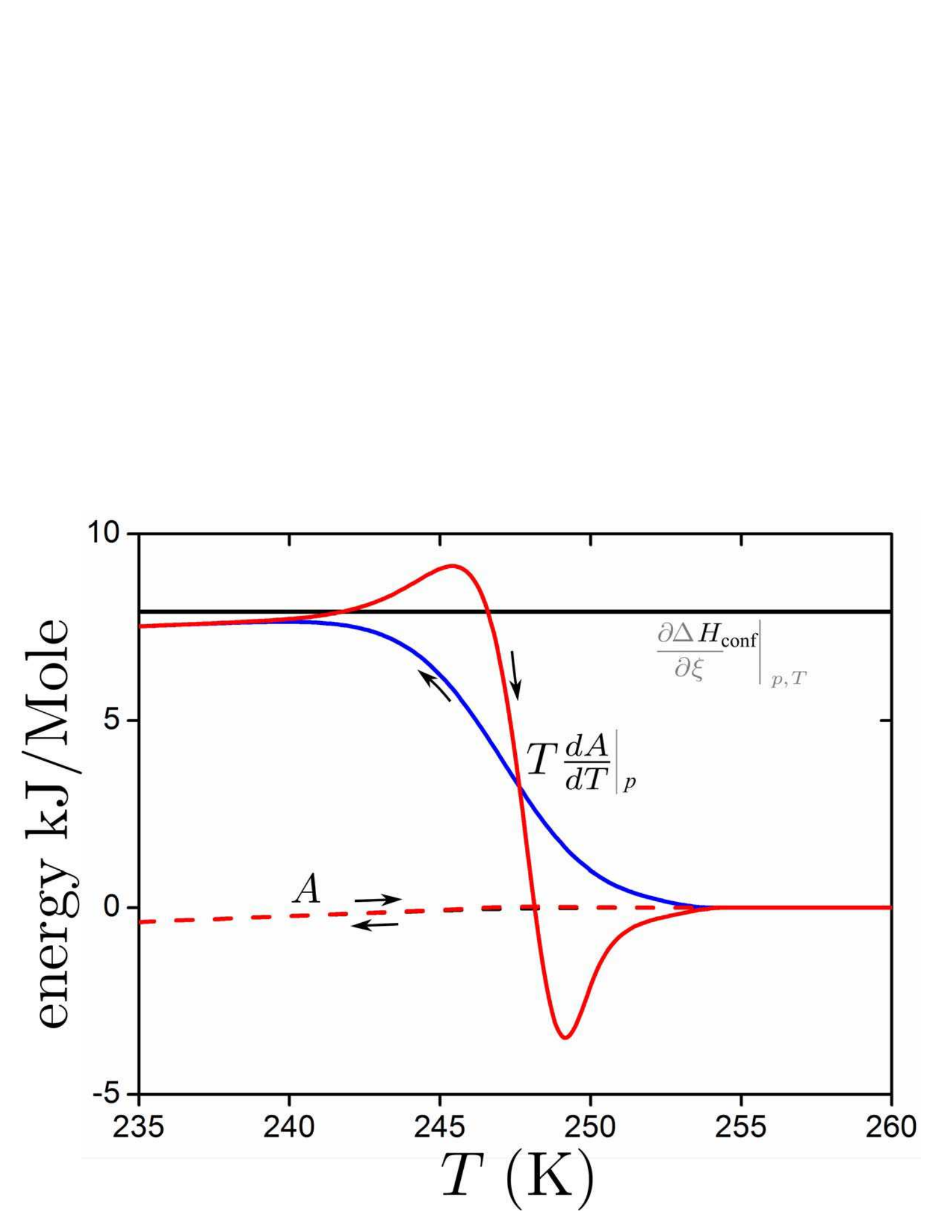
10
5
0
-5
235
240
245
250
255
260
energy kJ /Mole
T (K)
$\frac{\partial \Delta H_{\text{conf}}}{\partial \xi}\Big|_{p,T}$
$T\frac{dA}{dT}\Big|_{p}$
A

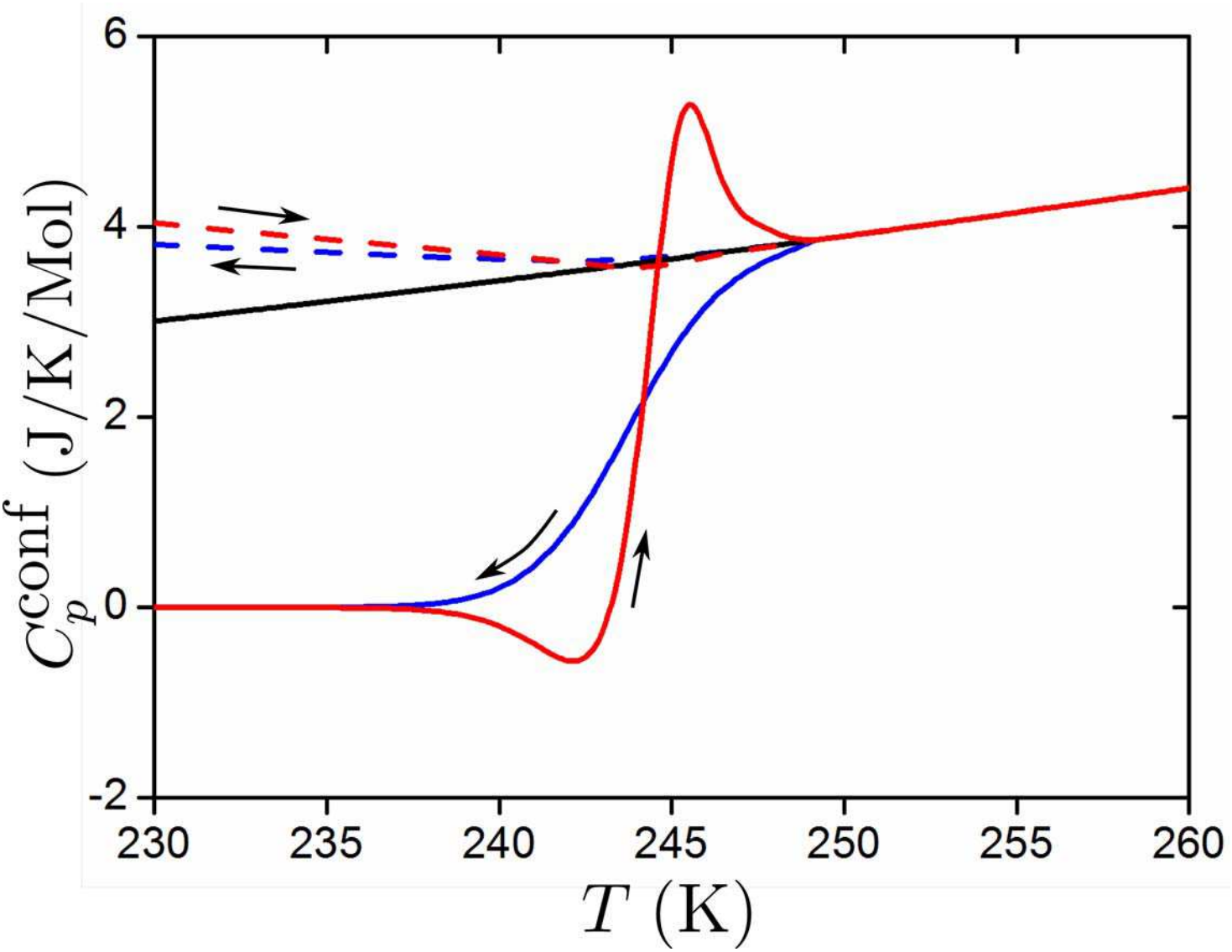
6
4
2
0
-2
230
235
240
245
250
255
260
C_p^{conf} (J/K/Mol)
T (K)

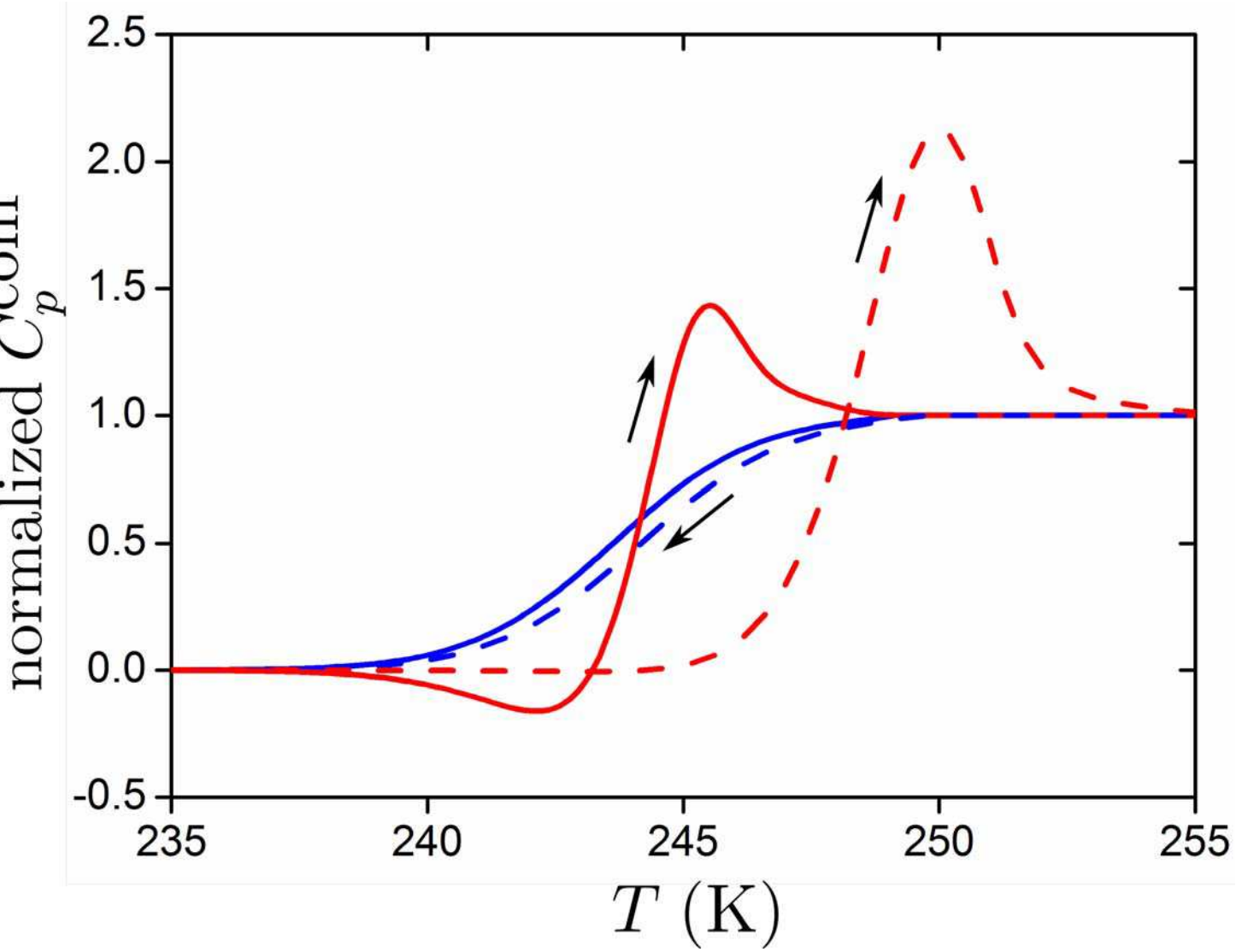
2.5
2.0
1.5
1.0
0.5
0.0
-0.5
normalized C_p^{conf}
235
240
245
250
255
T (K)

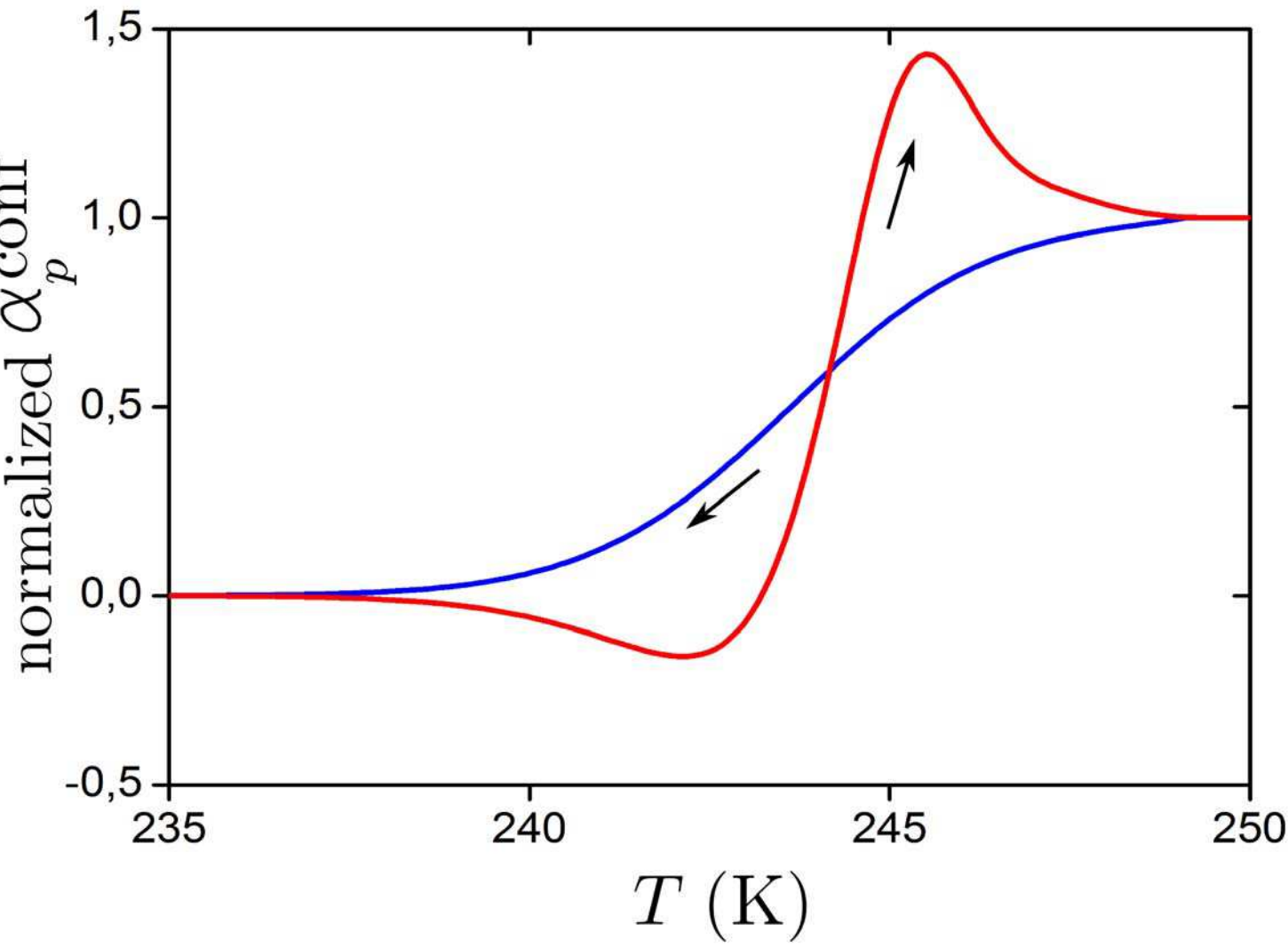
1,5
1,0
0,5
0,0
-0,5
normalized α_p^{conf}
235
240
245
250
T (K)

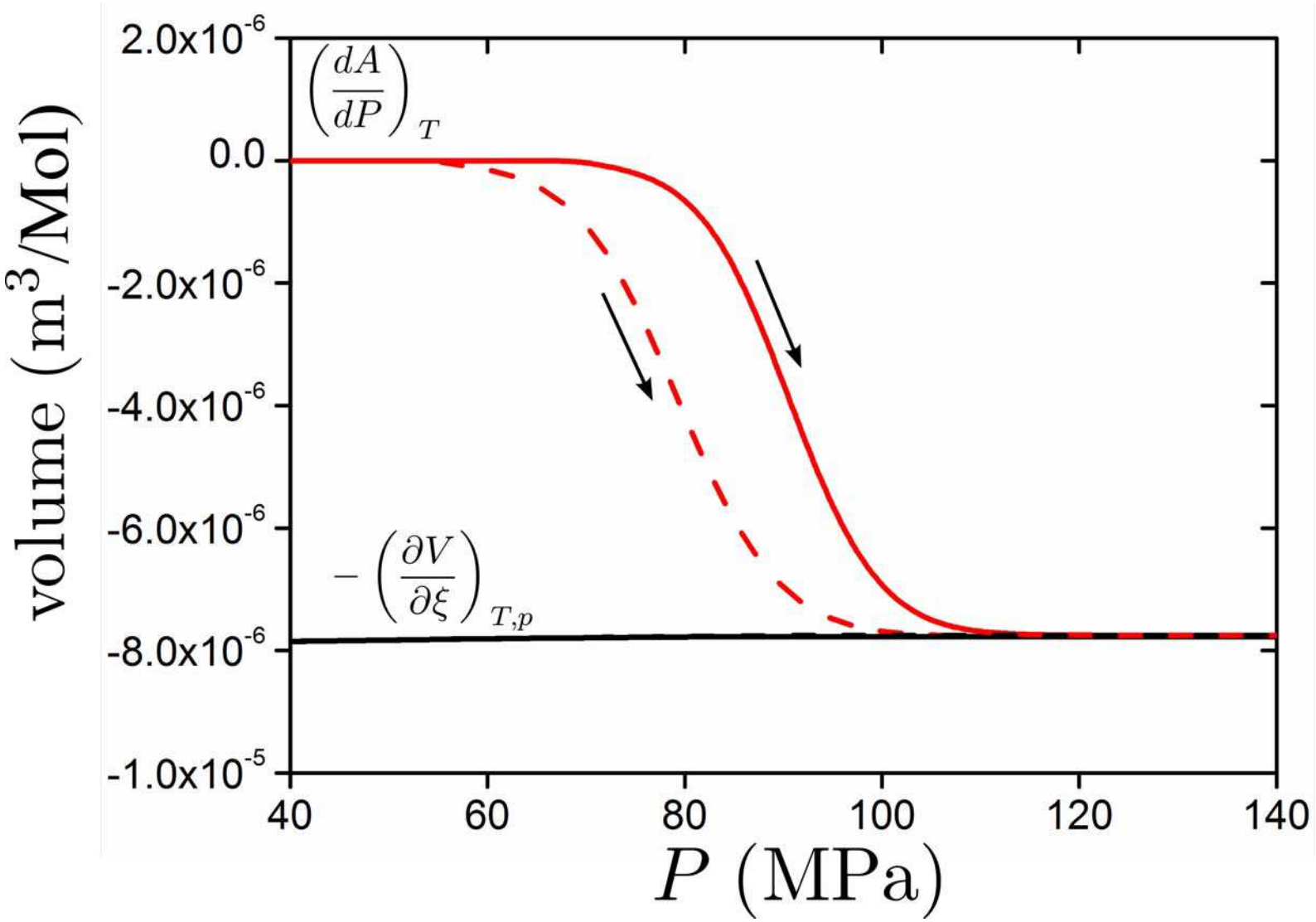
2.0x10-6
0.0
-2.0x10-6
-4.0x10-6
-6.0x10-6
-8.0x10-6
-1.0x10-5
volume (m3/Mol)
$\left(\frac{dA}{dP}\right)_T$
$-\left(\frac{\partial V}{\partial \xi}\right)_{T,p}$
40
60
80
100
120
140
P (MPa)

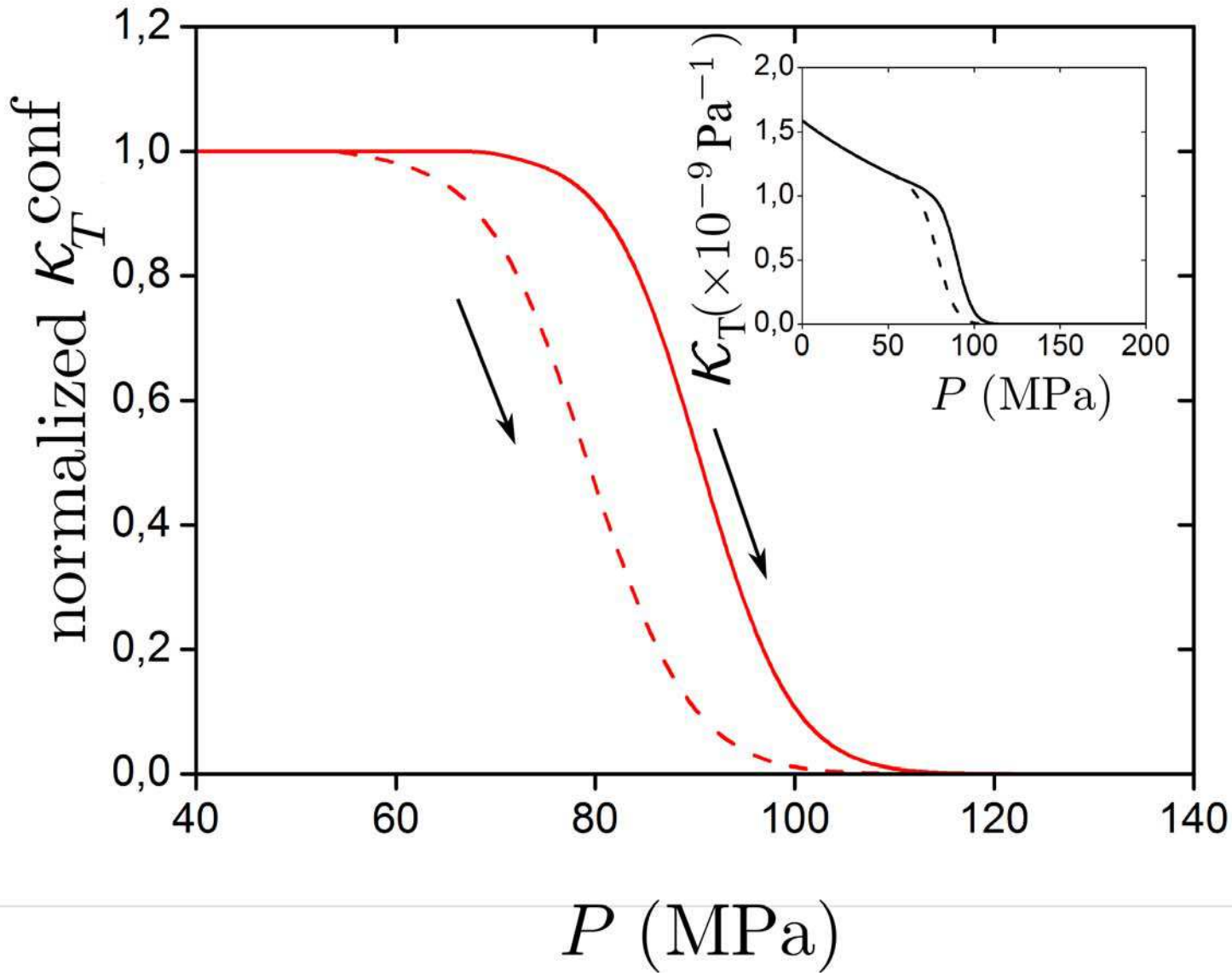
normalized κ_T^{conf}
1,2
1,0
0,8
0,6
0,4
0,2
0,0
40
60
80
100
120
140
P (MPa)
$\kappa_T (\times 10^{-9}\,\mathrm{Pa}^{-1})$
2,0
1,5
1,0
0,5
0,0
0
50
100
150
200
P (MPa)

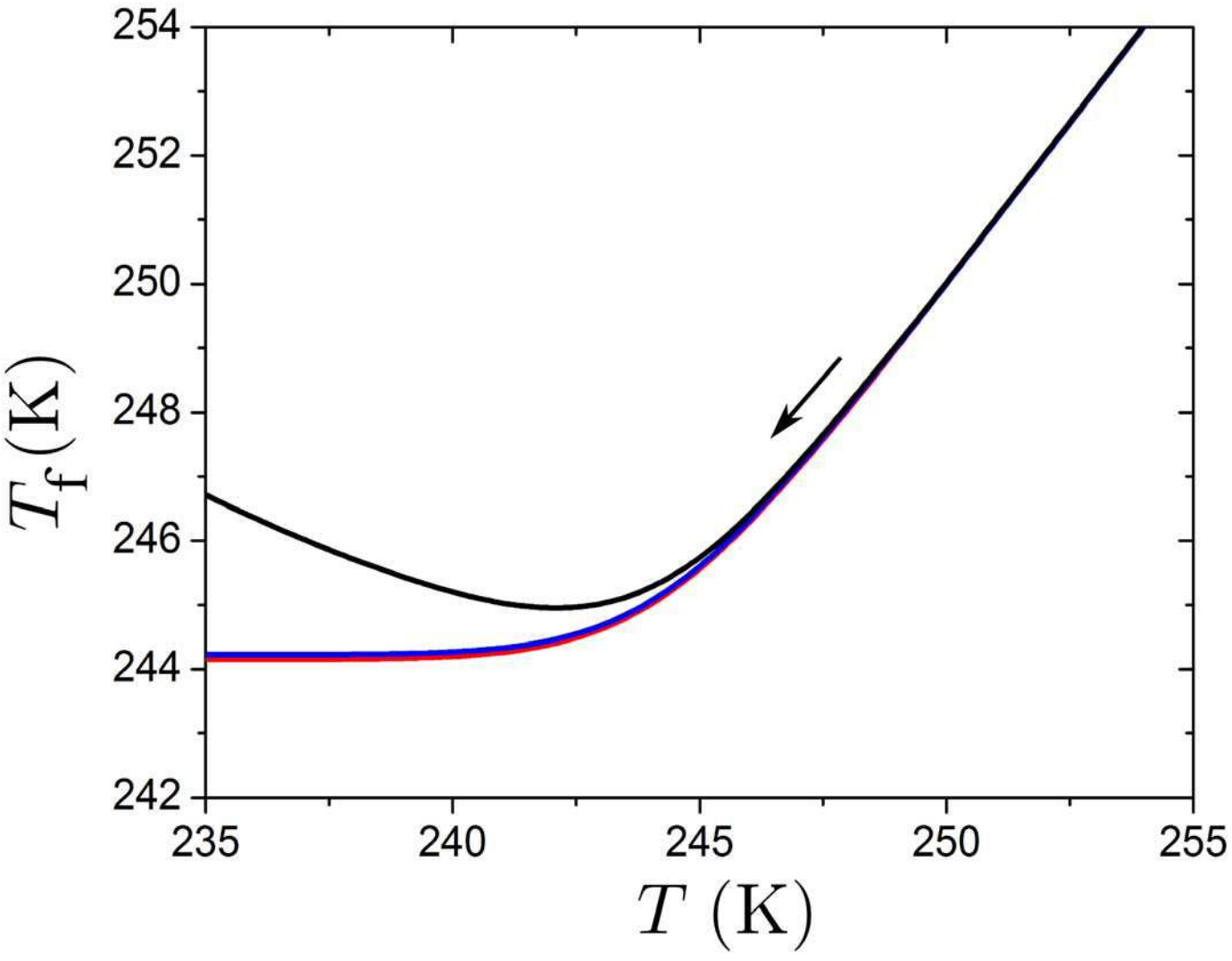
254
252
250
248
246
244
242
235
240
245
250
255
$T_{\mathrm{f}}\,(\mathrm{K})$
$T\ (\mathrm{K})$